Study of $B_c^+ \to J/\psi D_s^+$ and $B_c^+ \to J/\psi D_s^{*+}$ decays in pp collisions at $\sqrt{s} = 13$ TeV with the ATLAS detector

The ATLAS collaboration

E-mail: atlas.publications@cern.ch

ABSTRACT: A study of $B_c^+ \to J/\psi D_s^+$ and $B_c^+ \to J/\psi D_s^{*+}$ decays using $139\,\mathrm{fb}^{-1}$ of integrated luminosity collected with the ATLAS detector from $\sqrt{s} = 13\,\mathrm{TeV}$ *pp* collisions at the LHC is presented. The ratios of the branching fractions of the two decays to the branching fraction of the $B_c^+ \to J/\psi\pi^+$ decay are measured: $\mathcal{B}(B_c^+ \to J/\psi D_s^+)/\mathcal{B}(B_c^+ \to J/\psi\pi^+) = 2.76 \pm 0.47$ and $\mathcal{B}(B_c^+ \to J/\psi D_s^{*+})/\mathcal{B}(B_c^+ \to J/\psi\pi^+) = 5.33 \pm 0.96$. The ratio of the branching fractions of the two decays is found to be $\mathcal{B}(B_c^+ \to J/\psi D_s^{*+})/\mathcal{B}(B_c^+ \to J/\psi D_s^+) = 1.93 \pm 0.26$. For the $B_c^+ \to J/\psi D_s^{*+}$ decay, the transverse polarization fraction, $\Gamma_{\pm\pm}/\Gamma$, is measured to be 0.70 ± 0.11. The reported uncertainties include both the statistical and systematic components added in quadrature. The precision of the measurements exceeds that in all previous studies of these decays. These results supersede those obtained in the earlier ATLAS study of the same decays with $\sqrt{s} = 7$ and $8\,\mathrm{TeV}$ *pp* collision data. A comparison with available theoretical predictions for the measured quantities is presented.

Contents

1   Introduction

The large amount of pp collision data collected by the LHC experiments at a centre-of-mass energy $\sqrt{s} = 13$ TeV between 2015 and 2018 (Run 2) opens new opportunities to measure the properties of B_c^+ mesons precisely. Previous studies were limited by the low B_c^+ production cross-section. Being the only weakly decaying meson consisting of two heavy quarks, the B_c^+ meson provides a unique testing ground for various theoretical approaches that are used to describe its production and decays. In particular, the B_c^+ decays can occur through a weak transition of either heavy quark as well as through a weak annihilation.

Decays of B_c^+ to final states with a J/ψ meson involve a $\bar{b}$-quark transition, with the c-quark being a spectator. There is also a contribution from an annihilation diagram. Examples of the corresponding diagrams for the $B_c^+ \to J/\psi D_s^+$ and $B_c^+ \to J/\psi D_s^{*+}$ decays are shown in figure 1.

These decays were first observed by the LHCb experiment [1] and later by ATLAS [2] using data collected at centre-of-mass energies $\sqrt{s} = 7$ and 8 TeV in 2011–2012 (Run 1). Various predictions of their properties exist in theoretical works [3–12]. Only calculations in refs. [9, 12] explicitly account for small contributions from the annihilation diagram (figure 1(c)) to the $B_c^+ \to J/\psi D_s^{(*)+}$ decay amplitudes.

This paper presents a new study of these decays with the ATLAS detector [13]. It is based on pp collision data collected at $\sqrt{s} = 13$ TeV during Run 2 of the LHC, corresponding to an integrated luminosity of 139 fb^{-1}. The purpose of the new measurement is to improve
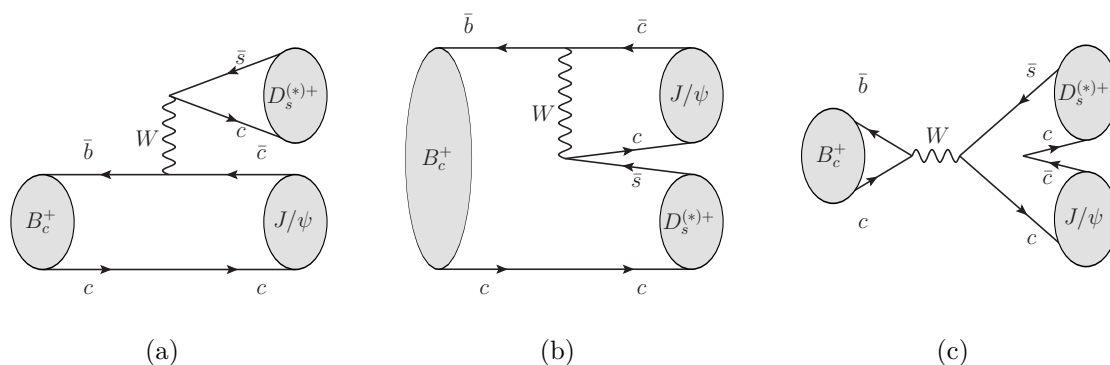
Figure 1. Feynman diagrams for $B_c^+ \to J/\psi D_s^{(*)+}$ decays: (a) colour-favoured spectator, (b) colour-suppressed spectator, and (c) annihilation topology.

the precision of measured properties of these decays by using a larger data sample and new analysis methods. In particular, a technique using boosted decision trees is applied to improve the signal decay candidate selection.

Similarly to ref. [2], the D_s^+ meson is reconstructed via the $D_s^+ \to \phi\pi^+$ decay, with the ϕ meson decaying into a pair of charged kaons. The D_s^{*+} meson decays into a D_s^+ meson and a soft photon or π^0 which is not reconstructed in the analysis. However, the mass difference between the D_s^{*+} and D_s^+ mesons is sufficient for the two decay signals to be resolved as two distinct structures in the distribution of the reconstructed mass of the $J/\psi D_s^+$ system. The J/ψ meson is reconstructed via its decay into a muon pair.

The $B_c^+ \to J/\psi\pi^+$ decay is used as a reference to measure the branching fractions. The following ratios are measured: $R_{D_s^+/\pi^+} = \mathcal{B}(B_c^+ \to J/\psi D_s^+)/\mathcal{B}(B_c^+ \to J/\psi\pi^+)$, $R_{D_s^{*+}/\pi^+} = \mathcal{B}(B_c^+ \to J/\psi D_s^{*+})/\mathcal{B}(B_c^+ \to J/\psi\pi^+)$, and $R_{D_s^{*+}/D_s^+} = \mathcal{B}(B_c^+ \to J/\psi D_s^{*+})/\mathcal{B}(B_c^+ \to J/\psi D_s^+)$.

The $B_c^+ \to J/\psi D_s^{*+}$ decay, being a transition of a pseudoscalar meson into two vector states, can be described in terms of three helicity amplitudes: A_{++}, A_{00} and A_{--}, where the indices correspond to the helicities of the J/ψ and D_s^{*+} mesons. The contribution of the A_{++} and A_{--} amplitudes, referred to as the $A_{\pm\pm}$ component, corresponds to the J/ψ and D_s^{*+} transverse polarization. Its fraction, $\Gamma_{\pm\pm}/\Gamma$, is also measured.

2 The ATLAS detector, data and simulated samples

The ATLAS detector[1] consists of three main components: an inner detector (ID) tracking system immersed in a 2 T axial magnetic field, surrounded by electromagnetic and hadronic calorimeters and by the muon spectrometer (MS). A full description of the detector can be

---

[1]ATLAS uses a right-handed coordinate system with its origin at the nominal interaction point (IP) in the centre of the detector and the z-axis along the beam pipe. The x-axis points from the IP to the centre of the LHC ring, and the y-axis points upward. Cylindrical coordinates (r, ϕ) are used in the transverse plane, ϕ being the azimuthal angle around the z-axis and r the distance from the IP in the transverse plane. The pseudorapidity is defined in terms of the polar angle θ as $\eta = -\ln\tan(\theta/2)$. Angular distance is measured in units of $\Delta R \equiv \sqrt{(\Delta\eta)^2 + (\Delta\phi)^2}$.

found in ref. [13], complemented by ref. [14] for details about the innermost silicon pixel layer that was installed for Run 2.

This analysis is based on the full Run 2 dataset of $\sqrt{s} = 13\,\text{TeV}$ pp collisions collected by ATLAS between 2015 and 2018 at the LHC. The data were recorded during stable LHC beam periods. Data quality requirements were imposed, notably on the performance of the MS and ID systems [15]. After applying these criteria, the integrated luminosity of the dataset amounts to $139\,\text{fb}^{-1}$, with an uncertainty of 1.7% [16], obtained using the LUCID-2 detector [17] for the primary luminosity measurements.

The data were collected during periods with different instantaneous luminosities, so several trigger configurations were used in the analysis to maximize the signal yields. Most of the triggers were based on identification of two muons, with various muon transverse momentum (p_T) thresholds (usually 4 and $6\,\text{GeV}$), requiring the oppositely charged muons in the pair to form a good vertex and have an invariant mass compatible with being produced by a $J/\psi \to \mu^+\mu^-$ decay. Since the event rate from these triggers was too high, prescale factors were applied to reduce it during periods with high instantaneous luminosity. To allow lower thresholds while keeping acceptable rates, other triggers required the presence of a third muon, which may appear in a semileptonic decay of hadrons containing b and $\bar{c}$ quarks present in an event along with the B_c^+ meson. Another set of triggers fitted a common vertex to two muons and two additional ID tracks, applying an invariant mass selection that assumed the $B_s^0 \to \mu^+\mu^-\phi$ decay topology. The events selected by these triggers require a special treatment described in section 4.

To model the inelastic pp events containing B_c^+ decays, large samples of Monte Carlo (MC) simulated events were prepared using the dedicated generator BCVEGPY 2.2 [18] interfaced to PYTHIA 8.244 [19] to simulate the parton showers and hadronization, and EVT-GEN [20] to model heavy-flavour decays. Simulated distributions of $p_\text{T}(B_c^+)$ and $|\eta(B_c^+)|$ were corrected to match the corresponding spectra of B_c^+ mesons in data, following the procedure described in section 6. The generated events with at least two muons having transverse momenta $p_\text{T}(\mu) > 3.5\,\text{GeV}$ and pseudorapidities $|\eta(\mu)| < 2.8$ were passed through a full simulation of the detector using the ATLAS simulation [21] based on GEANT4 [22]. A simulation of the triggers and their prescale factors was applied to all MC event samples used in the analysis.

An extensive software suite [23] is used in the reconstruction and analysis of real and simulated data, in detector operations, and in the trigger and data acquisition systems of the experiment.

3 Reconstruction and candidate selection

3.1 J/ψ candidates

The J/ψ candidates are built from pairs of oppositely charged muon candidates that are reconstructed using information from the MS and the ID. Muon candidates must satisfy the *Loose* identification working point [24]. The muon track parameters are determined from the ID measurement alone, since the precision of the measured track parameters is dominated by the ID track reconstruction in the p_T range of interest for this analysis. Pairs

of oppositely charged muon tracks are re-fitted to a common vertex. The quality of the vertex fit is required to satisfy $\chi^2 < 10$, where χ^2 is the fit quality (the number of degrees of freedom $N_{\mathrm{dof}} = 1$). This loose selection requirement is chosen to minimize biasing the χ^2 distribution of further cascade fit. The candidates in the dimuon invariant mass window $2800\,\mathrm{MeV} < m(\mu^+\mu^-) < 3400\,\mathrm{MeV}$ are retained for further analysis.

3.2 $B_c^+ \to J/\psi D_s^{(*)+}$ candidates

Candidate D_s^+ mesons from the $B_c^+ \to J/\psi D_s^{(*)+}$ decays[2] are reconstructed using the decay $D_s^+ \to \phi\pi^+$ with $\phi \to K^+K^-$. Oppositely charged particle tracks are assigned the kaon mass and combined in pairs to form ϕ candidates. Any additional track is assigned the pion mass and combined with the ϕ candidate to form a D_s^+ candidate. Only three-track combinations successfully fitted to a common vertex with $\chi^2/N_{\mathrm{dof}} < 5$ ($N_{\mathrm{dof}} = 3$) are accepted for further analysis. The invariant mass of the ϕ candidate, $m(K^+K^-)$, is required to be within a $\pm 7\,\mathrm{MeV}$ range around the world average ϕ mass, $m_\phi = 1019.461\,\mathrm{MeV}$ [25]. The D_s^+ candidate must have an invariant mass, $m(K^+K^-\pi^+)$, between $1930\,\mathrm{MeV}$ and $2010\,\mathrm{MeV}$, which spans about ± 2.5 standard deviations of the detector's mass resolution.

The $B_c^+ \to J/\psi D_s^{(*)+}$ candidates are built by combining the selected J/ψ and D_s^+ candidates. The J/ψ meson decays instantly at the same point as the B_c^+ meson does, whereas the D_s^+ meson lives long enough to form another displaced vertex. Following this cascade topology, a two-vertex fit is performed and the D_s^+ candidate's momentum is required to point back to the B_c^+ vertex [26]. To improve the mass resolution, the invariant masses of the J/ψ and D_s^+ candidates are constrained to the world average measured masses of the J/ψ and D_s^+ mesons [25], respectively.

In what follows, the B_c^+ invariant mass, $p_{\mathrm{T}}(B_c^+)$ and $\eta(B_c^+)$ are calculated using parameters of the tracks from the B_c^+ cascade vertex fit. The B_c^+ candidates are required to have $p_{\mathrm{T}}(B_c^+) > 15\,\mathrm{GeV}$ and $|\eta(B_c^+)| < 2.0$. The re-fitted muon tracks must have $p_{\mathrm{T}} > 4\,\mathrm{GeV}$ and $|\eta| < 2.3$, while the re-fitted hadron tracks are required to satisfy the $p_{\mathrm{T}} > 1\,\mathrm{GeV}$ and $|\eta| < 2.5$ requirements. The following preselection requirements are used to remove combinatorial background from the sample:

- $\chi^2(B_c^+)/N_{\mathrm{dof}} < 2$, where $\chi^2(B_c^+)$ is the quality of the B_c^+ cascade vertex fit and $N_{\mathrm{dof}} = 8$.

- $L_{xy}(B_c^+) > 0.3\,\mathrm{mm}$, where $L_{xy}(B_c^+)$ is the transverse distance between the B_c^+ candidate production vertex, which corresponds to the primary vertex of the pp interaction (PV), and its decay vertex projected onto the direction of the B_c^+ transverse momentum. As an event can contain several PVs, the actual PV is chosen as the one giving the smallest three-dimensional impact parameter of the B_c^+ candidate. To avoid biasing L_{xy}, the PV position is recalculated after removing any tracks used in the reconstruction of the B_c^+ meson candidate. To remove poorly reconstructed candidates, $L_{xy}(B_c^+)$ is also required to not exceed $10\,\mathrm{mm}$.

---

[2]The analysis considers both B_c^+ and B_c^- meson decays. For simplicity, charge conjugated states are implied from here onwards.

- $L_{xy}(D_s^+) > 0\,\text{mm}$, where $L_{xy}(D_s^+)$ is the transverse distance between the B_c^+ decay vertex and the D_s^+ decay vertex projected onto the direction of the D_s^+ transverse momentum. To remove poorly reconstructed candidates, $L_{xy}(D_s^+)$ is also required to not exceed $10\,\text{mm}$.

- $|d_0^{\text{PV}}(B_c^+)/\sigma_{d_0^{\text{PV}}}(B_c^+)| < 5$ and $|z_0^{\text{PV}}(B_c^+)/\sigma_{z_0^{\text{PV}}}(B_c^+)| < 5$, where d_0^{PV} and z_0^{PV} are the transverse and longitudinal impact parameters with respect to the PV, and $\sigma_{d_0^{\text{PV}}}(B_c^+)$ and $\sigma_{z_0^{\text{PV}}}(B_c^+)$ are their respective uncertainties. The uncertainties are calculated from the covariance matrix of the PV and the covariance matrix of the B_c^+ pseudo-track extracted from the cascade vertex fit. These two requirements are used to ensure that the B_c^+ candidate points back to the PV.

- $p_{\text{T}}(B_c^+)/\sum p_{\text{T}}(\text{trk}) > 0.10$, where the sum is taken over all tracks originating from the selected PV, including the tracks of the B_c^+ candidate. Due to the characteristic hard fragmentation of b-quarks, this requirement removes a sizeable fraction of the combinatorial background while having almost no effect on the signal.

Among various possible exclusive background contributions from $B \to J/\psi X$ decays, the only significant one was found to arise from the $B_s^0 \to J/\psi\phi$ process. Combining the tracks from a true $B_s^0 \to J/\psi\phi$, $J/\psi \to \mu^+\mu^-$, $\phi \to K^+K^-$ decay with another, random, track may produce a fake B_c^+ candidate. To suppress background events of this type, the $B_c^+ \to J/\psi D_s^{(*)+}$ candidates with $5340 < m(J/\psi\phi) < 5400\,\text{MeV}$ are rejected.

To further suppress the combinatorial background, a multivariate classifier based on boosted decision trees (BDTs) as implemented in the TMVA framework [27] is employed. The input variables used to train the classifier are the p_{T} of the D_s^+ meson candidate, the $L_{xy}(D_s^+)$ variable, and four angular variables:

- $\cos\theta^*(\pi^+)$, where $\theta^*(\pi^+)$ is the angle between the pion momentum in the $K^+K^-\pi^+$ rest frame and the $K^+K^-\pi^+$ combined momentum in the laboratory frame. The signal distribution of $\cos\theta^*(\pi^+)$ is flat before kinematic selection because the pseudoscalar D_s^+ meson decays isotropically, but it increases as $\cos\theta^*(\pi^+)$ approaches $+1$ for the background events.

- $|\cos^3\theta'(K^+)|$, where $\theta'(K^+)$ is the angle between one of the kaons and the pion in the K^+K^- rest frame. The decay of the pseudoscalar D_s^+ meson to the ϕ (vector) plus π^+ (pseudoscalar) final state results in the spin of the ϕ meson being aligned perpendicularly to the direction of motion of the ϕ relative to the D_s^+. Consequently, the distribution of $\cos\theta'(K)$ follows a $\cos^2\theta'(K)$ shape, implying a uniform distribution for $\cos^3\theta'(K)$. In contrast, the $\cos\theta'(K)$ distribution of the combinatorial background is approximately uniform and its $\cos^3\theta'(K)$ distribution peaks at zero.

- $\cos\theta^*(D_s^+)$, where $\theta^*(D_s^+)$ is the angle between the D_s^+ momentum in the B_c^+ rest frame and the B_c^+ flight direction in the laboratory frame. The distribution of $\cos\theta^*(D_s^+)$ is uniform for the decays of pseudoscalar B_c^+ mesons before kinematic selection, while it tends to increase towards negative values for the background.

- $\cos\theta'(\pi^+)$, where $\theta'(\pi^+)$ is the angle between the J/ψ momentum and the pion momentum in the $K^+K^-\pi^+$ rest frame. Its distribution is nearly uniform for the signal processes but peaks towards -1 and $+1$ for the background.

The information about the helicity in the $B_c^+ \to J/\psi D_s^{*+}$ decay is encoded in the J/ψ D_s^+ mass spectrum and in the distribution of $|\cos\theta'(\mu^+)|$, where $\theta'(\mu^+)$ is the helicity angle defined in the rest frame of the muon pair as the angle between the μ^+ and D_s^+ candidate momenta. It was verified that neither $m(J/\psi D_s^+)$ nor $|\cos\theta'(\mu^+)|$ is significantly correlated with the BDT input variables.

The BDT classifier is trained using signal candidates from the simulated samples and background candidates from the sidebands of the $J/\psi D_s^+$ system's mass distribution, defined as the union of the [5680, 5900] MeV and [6400, 6800] MeV ranges. No significant difference in the BDT output is observed when it is trained using either the $B_c^+ \to J/\psi D_s^+$ or $B_c^+ \to J/\psi D_s^{*+}$ signal sample, so the classifier used for the following selection is trained using both.

The ranges of the mass sidebands used to train the BDT were varied to ensure that the classifier does not produce a bias in the mass distribution: the training is repeated using either the inner or the outer halves of both sidebands, as well as using only the right sideband. Alternatively, the classifier trained with the nominal sidebands was applied to the $B_c^+ \to J/\psi D_s^{(*)+}$ candidates with $\chi^2(B_c^+)/N_{\rm dof} > 4$, where the signal contribution is expected to be negligible. No significant shaping of the $m(J/\psi D_s^+)$ distribution was found in these tests.

The cutting threshold set on the BDT output is chosen to maximize the significance $S/\sqrt{S+B}$, where S and B are the expected yields of signal and background events in the range $5900\,\text{MeV} < m(J/\psi D_s^+) < 6350\,\text{MeV}$. Following the optimization procedure, a threshold value corresponding to the efficiency of 81% is chosen.

Candidates within the mass range $5680\,\text{MeV} < m(J/\psi D_s^+) < 6800\,\text{MeV}$ are retained for further analysis. If more than one candidate in an event passes the selection (this happens in about 10% of events with at least one passing candidate), all of them are kept.

3.3 $B_c^+ \to J/\psi\pi^+$ candidates

To reconstruct the $B_c^+ \to J/\psi\pi^+$ candidates, a J/ψ candidate is combined with an additional charged-particle track which is assigned the pion mass. For the pion candidate, tracks identified as muons passing the *low-p_T* identification working point [24] are vetoed in order to suppress a substantial background from $B_c^+ \to J/\psi\mu^+\nu_\mu X$ decays. The three-track combination is re-fitted to a common vertex, with the J/ψ candidate mass constrained to the world average value [25].

In what follows, the B_c^+ invariant mass, $p_T(B_c^+)$ and $\eta(B_c^+)$ are calculated using the track parameters from the B_c^+ candidate vertex fit. The B_c^+ candidates are required to have $p_T(B_c^+) > 15\,\text{GeV}$ and $|\eta(B_c^+)| < 2.0$. The re-fitted muon tracks must have $p_T > 4\,\text{GeV}$ and $|\eta| < 2.3$, while the re-fitted pion track is required to satisfy $p_T > 3.5\,\text{GeV}$ and $|\eta| < 2.5$. To suppress combinatorial background the following requirements are used:

- $\chi^2(B_c^+)/N_{\rm dof} < 1.8$ ($N_{\rm dof} = 4$ in the $B_c^+ \to J/\psi \pi^+$ vertex fit),

- $L_{xy}(B_c^+) > 0.3 \,\mathrm{mm}$,

- $|d_0^{\rm PV}(B_c^+)/\sigma_{d_0^{\rm PV}}(B_c^+)| < 3$ and $|z_0^{\rm PV}(B_c^+)/\sigma z_0^{\rm PV}(B_c^+)| < 3$,

- $p_{\rm T}(B_c^+)/\sum p_{\rm T}({\rm trk}) > 0.10$,

where the definitions of all these variables for the $B_c^+ \to J/\psi \pi^+$ candidates are the same as the corresponding ones for the $B_c^+ \to J/\psi D_s^{(*)+}$ selection.

Candidates within the mass range $5800 \,\mathrm{MeV} < m(J/\psi \pi^+) < 7100 \,\mathrm{MeV}$ are retained for further analysis. If more than one candidate in an event passes the selection, all of them are kept.

4 Signal parameters extraction

As described in section 2, various types of trigger selection chains were used to collect the events for the analysis. Most of them are based on identification of muons from $J/\psi \to \mu^+\mu^-$ decays and hence are equally efficient for $B_c^+ \to J/\psi D_s^{(*)+}$ and $B_c^+ \to J/\psi \pi^+$ decay events. However, one suite of triggers attempts to reconstruct $\mu^+\mu^-\phi(K^+K^-)$ candidates; these triggers, originally intended for the collection of $B_s^0 \to \mu^+\mu^-\phi$ events [28], are not efficient for the reference decay events and may produce a bias in measurements using this channel. Nevertheless, they contribute significantly to the $B_c^+ \to J/\psi D_s^{(*)+}$ signal yields and can be used to measure the quantities related exclusively to these decays, namely the ratio of branching fractions $R_{D_s^{*+}/D_s^+}$ and the transverse polarization fraction $\Gamma_{\pm\pm}/\Gamma$.

To that end, all selected $B_c^+ \to J/\psi D_s^{(*)+}$ candidates are separated into two (non-overlapping) datasets:

- *Dataset 1*: candidates in the events collected by the standard dimuon triggers or by three-muon triggers without requirements on the additional ID tracks.

- *Dataset 2*: candidates collected only by the dedicated $B_s^0 \to \mu^+\mu^-\phi$ triggers and not by other ones used in the analysis.

The $R_{D_s^+/\pi^+}$ and $R_{D_s^{*+}/\pi^+}$ ratios are measured using only the $B_c^+ \to J/\psi D_s^{(*)+}$ decay yields in Dataset 1, while the full dataset, i.e. the union of Dataset 1 and Dataset 2, is employed for the $R_{D_s^{*+}/D_s^+}$ and $\Gamma_{\pm\pm}/\Gamma$ measurements. In the $B_c^+ \to J/\psi \pi^+$ signal yield extraction, the events collected by the $B_s^0 \to \mu^+\mu^-\phi$ triggers are not used at all.

4.1 Extraction of $B_c^+ \to J/\psi D_s^{(*)+}$ signal parameters

An extended unbinned maximum-likelihood fit to the two-dimensional distribution of $m(J/\psi D_s^+)$ and $|\cos\theta'(\mu^+)|$ is performed to extract the signal yields as well as the transverse polarization fraction in $B_c^+ \to J/\psi D_s^{*+}$ decays. The signal and background probability density functions (PDFs) for the fit are assumed to be uncorrelated in $m(J/\psi D_s^+)$ and $|\cos\theta'(\mu^+)|$ and can therefore be factorized into mass and angular parts. For the signals, this assumption was validated using the simulated samples. A small correlation ($\sim 1\%$)

was observed for the background, manifesting itself in a statistically insignificant difference between the $|\cos\theta'(\mu^+)|$ shapes of the left and right mass-sideband events; its effect is accounted for by assigning a systematic uncertainty.

As stated in section 1, the $B_c^+ \to J/\psi D_s^{*+}$ decay can be described in terms of three helicity amplitudes: A_{++}, A_{00}, and A_{--}. The $m(J/\psi D_s^+)$ and $|\cos\theta'(\mu^+)|$ spectra should be the same for the A_{++} and A_{--} amplitudes, and that is confirmed with the MC simulation. Therefore, the $B_c^+ \to J/\psi D_s^{*+}$ signal is described by a model with two helicity components corresponding to the $A_{\pm\pm}$ and A_{00} contributions.

Dataset 1 and Dataset 2 are fitted simultaneously. The MC simulation indicates that both the $m(J/\psi D_s^+)$ and $|\cos\theta'(\mu^+)|$ distributions of the $B_c^+ \to J/\psi D_s^+$ signal and of the helicity components of the $B_c^+ \to J/\psi D_s^{*+}$ signal are consistent between Dataset 1 and Dataset 2. Efficiency ratios between these signal components are consistent between Datasets 1 and 2 as well. Therefore, the signal shapes and all signal parameters (except the yields) extracted from the fit are treated as being the same in Dataset 1 and Dataset 2.

The $m(J/\psi D_s^+)$ and $|\cos\theta'(\mu^+)|$ shapes of the two helicity components of the $B_c^+ \to J/\psi D_s^{*+}$ signal are described using templates made from the MC simulated event samples with the adaptive kernel estimation technique [29]. The $A_{\pm\pm}$ component's fraction in the total $B_c^+ \to J/\psi D_s^{*+}$ reconstructed yield, $f_{\pm\pm}$, is a free parameter of the fit.

The $m(J/\psi D_s^+)$ PDF for the $B_c^+ \to J/\psi D_s^+$ signal is parameterized by a modified Gaussian function, G_{mod} [30, 31]:

$$G_{\text{mod}} \propto \exp\left(-0.5 \times t^{1+1/(1+t/2)}\right), \tag{4.1}$$

where $t = |m(J/\psi D_s^+) - m_{B_c^+}|/\sigma_{B_c^+}$ with the mean mass $m_{B_c^+}$ and width $\sigma_{B_c^+}$ being free parameters of the fit. The $B_c^+ \to J/\psi D_s^+$ signal's angular PDF is also determined from the MC simulated events by using the adaptive kernel estimation technique.

Second-order polynomial shapes are used to describe the background $|\cos\theta'(\mu^+)|$ PDFs for Dataset 1 and Dataset 2, while the mass PDFs are parameterized by exponential functions. The parameters of these polynomial and exponential shapes are allowed to float independently for Dataset 1 and Dataset 2.

The free parameters of the fit also include the ratio of the $B_c^+ \to J/\psi D_s^{*+}$ yield to the $B_c^+ \to J/\psi D_s^+$ yield, $r_{D_s^{*+}/D_s^+}$, and the $B_c^+ \to J/\psi D_s^+$ signal yields in Datasets 1 and 2, $N_{B_c^+ \to J/\psi D_s^+}^{\text{DS1}}$ and $N_{B_c^+ \to J/\psi D_s^+}^{\text{DS2}}$. The values of the signal parameters obtained from the fit to the data are shown in table 1. It also shows the $B_c^+ \to J/\psi D_s^{*+}$ signal yield in Dataset 1, $N_{B_c^+ \to J/\psi D_s^{*+}}^{\text{DS1}}$, and the yields of both signals in the full dataset, $N_{B_c^+ \to J/\psi D_s^+}^{\text{DS1\&2}}$ and $N_{B_c^+ \to J/\psi D_s^{*+}}^{\text{DS1\&2}}$; their values and uncertainties are calculated from the parameter values and covariance matrix obtained from the fit. The fitted B_c^+ mass is in good agreement with the world average value [25] and the width agrees with the MC simulation. The projections of the two-dimensional fit onto Dataset 1 and Dataset 2 are shown in figure 2.

4.2 Fit of $B_c^+ \to J/\psi\pi^+$ candidates

The yield of the $B_c^+ \to J/\psi\pi^+$ decay signal is extracted with an extended unbinned maximum-likelihood fit to the distribution of $J/\psi\pi^+$ mass.
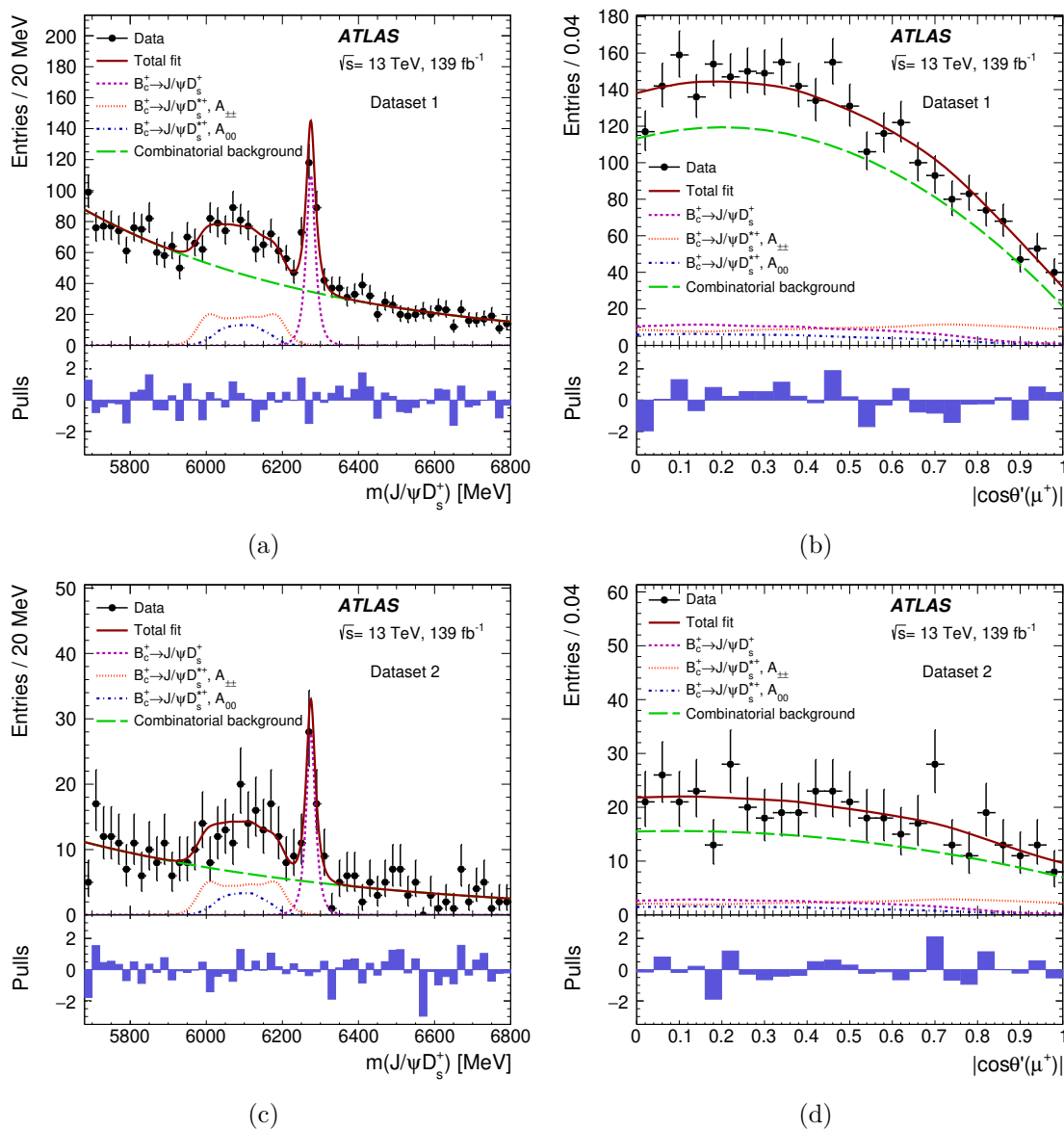
Figure 2. Distributions of ((a), (c)) the $J/\psi D_s^+$ mass and ((b), (d)) $|\cos\theta'(\mu^+)|$ for the selected $B_c^+ \to J/\psi D_s^{(*)+}$ candidates in ((a), (b)) Dataset 1 and ((c), (d)) Dataset 2. Data are shown as points, and the overall result of the fit is given by the red solid curve. The purple dashed line shows the contribution of the $B_c^+ \to J/\psi D_s^+$ signal, while the orange dotted and blue dashed-dotted lines show the contributions of the $A_{\pm\pm}$ and A_{00} components of the $B_c^+ \to J/\psi D_s^{*+}$ signal, respectively. The background contribution is shown with the green long-dashed line. The bottom panels show the pulls, defined as the difference between the data and the fit function divided by the uncertainty of the data point.

Parameter	Value
$m_{B_c^+}$ [MeV]	6274.8 ± 1.4
$\sigma_{B_c^+}$ [MeV]	11.5 ± 1.5
$r_{D_s^{*+}/D_s^+}$	1.76 ± 0.22
$f_{\pm\pm}$	0.70 ± 0.10
$N^{\mathrm{DS1}}_{B_c^+ \to J/\psi D_s^+}$	193 ± 20
$N^{\mathrm{DS2}}_{B_c^+ \to J/\psi D_s^+}$	49 ± 10
$N^{\mathrm{DS1}}_{B_c^+ \to J/\psi D_s^{*+}}$	338 ± 32
$N^{\mathrm{DS1\&2}}_{B_c^+ \to J/\psi D_s^+}$	241 ± 28
$N^{\mathrm{DS1\&2}}_{B_c^+ \to J/\psi D_s^{*+}}$	424 ± 46

Table 1. Parameters of the $B_c^+ \to J/\psi D_s^+$ and $B_c^+ \to J/\psi D_s^{*+}$ signals obtained with the unbinned extended maximum-likelihood fit to the data. Only the statistical uncertainties are included. No acceptance or efficiency corrections are applied to the signal yields.

In the fit, the signal is modelled by a modified Gaussian function, eq. (4.1), and the combinatorial background is described by a two-parameter exponential function, $\exp(-a_0 m \times (1 + a_1 m))$.

In addition to the combinatorial background, there is a significant contribution from partially reconstructed B_c^+ decays (PRDs), $B_c^+ \to J/\psi X$, where a charged-particle track from X can be reconstructed as a pion of the $B_c^+ \to J/\psi \pi^+$ candidate. The contribution of such decays can create structures in the left sideband of the $B_c^+ \to J/\psi \pi^+$ signal peak that could not be described by the smooth shape of the combinatorial background PDF. MC studies show that the dominant contribution to such decays comes from the $B_c^+ \to J/\psi \rho^+$ decay, with ρ^+ decaying into $\pi^+ \pi^0$, while other decays, if present, exhibit a fairly smooth dependence on $m(J/\psi \pi^+)$ that can be absorbed by the functional form used to model the combinatorial background.

The $B_c^+ \to J/\psi \rho^+$ decay is a transition of a pseudoscalar to two vector states and, similarly to $B_c^+ \to J/\psi D_s^{*+}$, can be described in terms of three helicity amplitudes. The contributions corresponding to the $A_{\pm\pm}$ and A_{00} amplitudes have a significantly different shape in $m(J/\psi \pi^+)$. Therefore, to model this background in the fit, templates for these two contributions are built out of simulated events, using adaptive kernel estimation technique, and added to the fit PDF, leaving their relative fraction a free parameter. The overall normalization of this PRD component is left free as well.

A small peaking background from CKM-suppressed $B_c^+ \to J/\psi K^+$ decay events, which behaves similarly to signal, is expected in data. The PDF for this contribution is obtained by applying the adaptive kernel estimation technique to a simulation of the $B_c^+ \to J/\psi K^+$ channel. The ratio of the $B_c^+ \to J/\psi K^+$ and $B_c^+ \to J/\psi \pi^+$ yields is fixed according to the reconstruction efficiencies (nearly equal for the two modes) and the relative branching fraction [25].

Parameter	Value
$m_{B_c^+}$ [MeV]	6274.5 ± 1.5
$\sigma_{B_c^+}$ [MeV]	47.5 ± 2.5
$N_{B_c^+ \to J/\psi \pi^+}$	8440^{+550}_{-470}

Table 2. Parameters of the $B_c^+ \to J/\psi \pi^+$ signal obtained with the unbinned extended maximum-likelihood fit. Only the statistical uncertainties are included. No efficiency correction is applied to the signal yield.
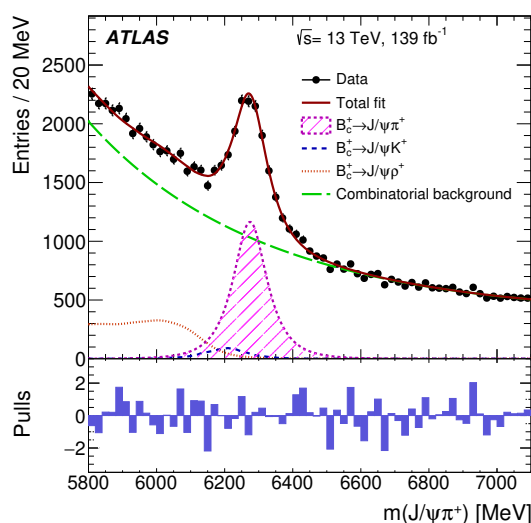

Figure 3. Distributions of the $J/\psi \pi^+$ mass for the selected $B_c^+ \to J/\psi \pi^+$ candidates. Data are shown as points, and the overall result of the fit is given by the red solid curve. The signal contribution is shown by the purple shaded area. The red dotted, blue dashed, and green long-dashed lines correspond to the $B_c^+ \to J/\psi \rho^+$, $B_c^+ \to J/\psi K^+$, and combinatorial background contributions, respectively. The bottom panel shows the pulls, defined as the difference between the data and the fit function divided by the uncertainty of the data point.

The mass and width of the $B_c^+ \to J/\psi \pi^+$ signal and its yield, $N_{B_c^+ \to J/\psi \pi^+}$, obtained from the fit are given in table 2. The fitted B_c^+ mass is in good agreement with the world average value [25] and the width agrees with the MC simulation. Figure 3 shows the measured $m(J/\psi \pi^+)$ distribution overlaid with the result of the fit and its signal and individual background components.

5 Measurement of the decay parameters

The ratio of the branching fractions of $B_c^+ \to J/\psi D_s^{(*)+}$ and $B_c^+ \to J/\psi \pi^+$ decays is given by

$$R_{D_s^{(*)+}/\pi^+} = \frac{\mathcal{B}(B_c^+ \to J/\psi D_s^{(*)+})}{\mathcal{B}(B_c^+ \to J/\psi \pi^+)} = \frac{N^{\mathrm{DS1}}_{B_c^+ \to J/\psi D_s^{(*)+}}}{N_{B_c^+ \to J/\psi \pi^+}} \times \frac{\epsilon_{B_c^+ \to J/\psi \pi^+}}{\epsilon^{\mathrm{DS1}}_{B_c^+ \to J/\psi D_s^{(*)+}}} \times \frac{1}{\mathcal{B}(D_s^+ \to \phi(K^+K^-)\pi^+)},$$

(5.1)

and the ratio of the branching fractions of $B_c^+ \to J/\psi D_s^{*+}$ and $B_c^+ \to J/\psi D_s^+$ is[3]

$$R_{D_s^{*+}/D_s^+} = \frac{\mathcal{B}(B_c^+ \to J/\psi D_s^{*+})}{\mathcal{B}(B_c^+ \to J/\psi D_s^+)} = \frac{N_{B_c^+ \to J/\psi D_s^{*+}}^{\mathrm{DS1\,2}}}{N_{B_c^+ \to J/\psi D_s^+}^{\mathrm{DS1\,2}}} \times \frac{\epsilon_{B_c^+ \to J/\psi D_s^+}^{\mathrm{DS1\,2}}}{\epsilon_{B_c^+ \to J/\psi D_s^{*+}}^{\mathrm{DS1\,2}}} = r_{D_s^{*+}/D_s^+} \times \frac{\epsilon_{B_c^+ \to J/\psi D_s^+}^{\mathrm{DS1\,2}}}{\epsilon_{B_c^+ \to J/\psi D_s^{*+}}^{\mathrm{DS1\,2}}}.$$

(5.2)

Here N and ϵ denote the yield and the total efficiency of the corresponding mode indicated in the subscripts. The superscript DS1 or DS1&2 defines whether the value corresponds to Dataset 1 or the full dataset, respectively.

The total efficiency is as a product of kinematic acceptance and reconstruction efficiency. The kinematic range of the measurement is defined in terms of the transverse momentum and pseudorapidity of the B_c^+ meson as $p_\mathrm{T}(B_c^+) > 15\,\mathrm{GeV}$ and $|\eta(B_c^+)| < 2.0$. The kinematic acceptance is defined as the fraction of the B_c^+ decay events in the kinematic range which pass the same requirements as those placed on the decay's muon and hadron tracks for the signal extraction. It is determined using large generator-level samples without applying a selection on the decay products. The reconstruction efficiency is evaluated using the MC simulation as the ratio of the number of events passing the full analysis selection to the number of events passing the B_c^+ and decay product requirements at generator level. The reconstruction efficiencies for Dataset 1 and for the full dataset are determined by requiring the simulated events to pass any of the triggers qouted in the Dataset 1 definition and any of the triggers used in the analysis, respectively.

For the value of the branching fraction $\mathcal{B}(D_s^+ \to \phi(K^+K^-)\pi^+)$ of the $D_s^+ \to \phi\pi^+$ decay followed by $\phi \to K^+K^-$, the CLEO measurement [32] of the partial $D_s^+ \to K^+K^-\pi^+$ branching fractions is used, with a kaon-pair mass within various intervals around the nominal ϕ meson mass. An interpolation between the partial branching fractions, measured in $\pm5\,\mathrm{MeV}$ and $\pm10\,\mathrm{MeV}$ intervals by using a relativistic Breit-Wigner distribution for the shape of the resonance, yields the value $(1.85 \pm 0.11)\%$ for the $\pm7\,\mathrm{MeV}$ interval which is used in the analysis. This is done as in ref. [2].

The total efficiencies for all decay modes are shown in table 3. They are different for the $A_{\pm\pm}$ and A_{00} components of the $B_c^+ \to J/\psi D_s^{*+}$ decay, hence the overall efficiency for this mode is given by

$$\epsilon_{B_c^+ \to J/\psi D_s^{*+}} = \frac{1}{f_{\pm\pm}/\epsilon_{B_c^+ \to J/\psi D_s^{*+}, A_{\pm\pm}} + (1 - f_{\pm\pm})/\epsilon_{B_c^+ \to J/\psi D_s^{*+}, A_{00}}},$$

which is valid for either Dataset 1 or the full dataset, and $f_{\pm\pm}$ has the value taken from the fit (shown in table 1).

The fraction of transverse polarization in the $B_c^+ \to J/\psi D_s^{*+}$ decay, $\Gamma_{\pm\pm}/\Gamma$, is the fraction of the $A_{\pm\pm}$ component and is calculated from the $f_{\pm\pm}$ value by applying a correction to account for the difference between the total efficiencies for the two component contributions:

$$\Gamma_{\pm\pm}/\Gamma = f_{\pm\pm} \times \frac{\epsilon_{B_c^+ \to J/\psi D_s^{*+}}^{\mathrm{DS1\&2}}}{\epsilon_{B_c^+ \to J/\psi D_s^{*+}, A_{\pm\pm}}^{\mathrm{DS1\&2}}}.$$

(5.3)

---

[3]It is assumed that $\mathcal{B}(D_s^{*+} \to D_s^+ X)$ is 100%.

Mode	ϵ^{DS1} [%]	$\epsilon^{\mathrm{DS1\&2}}$ [%]
$B_c^+ \to J/\psi D_s^+$	0.971 ± 0.012	1.163 ± 0.013
$B_c^+ \to J/\psi D_s^{*+}$, A_{00}	0.916 ± 0.012	1.088 ± 0.012
$B_c^+ \to J/\psi D_s^{*+}$, $A_{\pm\pm}$	0.868 ± 0.010	1.049 ± 0.011
$B_c^+ \to J/\psi \pi^+$	2.169 ± 0.018	—

Table 3. Summary of the total efficiencies. Quoted uncertainties correspond to statistical uncertainties of the simulated samples. For the $B_c^+ \to J/\psi\pi^+$ channel, the efficiency $\epsilon_{B_c^+ \to J/\psi\pi^+}$ entering the equations for $R_{D_s^{(*)+}/\pi^+}$ is shown, while the efficiency for the full dataset is not defined.

6 Systematic uncertainties

Various sources of systematic uncertainty are considered and outlined in this section. The systematic uncertainties can be classified into two categories. The first category relates to the possible differences between the data and MC simulation which affect the signal acceptances and reconstruction efficiencies. The second category includes the uncertainties in the signal extraction procedure, for both the $B_c^+ \to J/\psi D_s^{(*)+}$ and $B_c^+ \to J/\psi\pi^+$ channels. Each source of systematic uncertainty is considered individually by repeating the analysis with a certain systematic change implemented. The deviation from the nominal result is then symmetrized and assigned as the uncertainty. Although some sources can have rather large effects on the individual decay rate measurements, they largely cancel out in the ratios of the branching fractions due to correlations between their effects on the different decay modes.

The systematic uncertainties affecting the acceptances and reconstruction efficiencies are the following.

- *MC modelling of B_c^+ production.* To correct for the possible difference in B_c^+ kinematics between data and MC simulation, the $p_\mathrm{T}(B_c^+)$ and $|\eta(B_c^+)|$ spectra are extracted using the abundant $B_c^+ \to J/\psi\pi^+$ channel with an *sPlot* technique [33]. A linear fit of data/MC ratio for these spectra is performed and weights are assigned to simulated events according to the slope of the fitted linear function. This slope is varied in a range preserving one standard deviation agreement with data. The slopes are varied independently for the $p_\mathrm{T}(B_c^+)$ and $|\eta(B_c^+)|$ distributions. They affect both the kinematic acceptances and reconstruction efficiencies. The effects are found to be 1.5%–2% for $R_{D_s^{(*)+}/\pi^+}$ ratios and below 0.5% for $R_{D_s^{(*)+}/D_s^+}$ and $\Gamma_{\pm\pm}/\Gamma$.

- Limited knowledge of B_c^+ *and D_s^+ mesons lifetimes* leads to an additional systematic uncertainty due to different decay time acceptances between the B_c^+ decay modes. The effect is estimated by varying these lifetimes within the uncertainties of their world average values [25] and is found to be below 0.5% for $R_{D_s^{(*)+}/\pi^+}$ ratios.

- The *tracking efficiency uncertainty* is dominated by the uncertainty in the detector material description used in the MC simulation. It is estimated from independent

measurements of secondary vertices in the detector volume and results in an effect of about 1% for the $R_{D_s^{(*)+}/\pi^+}$ ratios and below 0.1% for $R_{D_s^{*+}/D_s^+}$ and $\Gamma_{\pm\pm}/\Gamma$.

- The effect of *uncertainties in the modelling of multiple proton-proton interactions (pile-up)* in MC simulation is estimated by correcting the MC pile-up profile to the profile in data. The effects on the $R_{D_s^{(*)+}/\pi^+}$ ratios are found to be about 1%, while those on $R_{D_s^{*+}/D_s^+}$ and $\Gamma_{\pm\pm}/\Gamma$ are statistically insignificant.

- The effect of possible mis-modelling of the *efficiency of χ^2/N_{dof} and impact parameter selection* is evaluated by comparing their distributions in simulation and data using the *sPlot* technique, independently for $B_c^+ \to J/\psi D_s^{(*)+}$ and $B_c^+ \to J/\psi\pi^+$ events. Good agreement is found, and weights are used to vary the simulated distribution, still preserving one standard deviation agreement with data. The effects on the $R_{D_s^{(*)+}/\pi^+}$ ratios are found to be 3.2% and 0.2% for the modelling of χ^2/N_{dof} and the impact parameters, respectively, with no significant effect on $R_{D_s^{*+}/D_s^+}$ and $\Gamma_{\pm\pm}/\Gamma$.

- The effect of an *uncertainty in the efficiency of the BDT selection* is evaluated in the same way, using the distribution of the BDT output variable. Very good agreement is found here as well, and variations preserving one standard deviation agreement with data estimate an effect of 1.3% for $R_{D_s^{(*)+}/\pi^+}$ ratios.

- The possible effect of mis-modelling the *trigger efficiency* is expected to be small because the same triggers are used to select events from the different decay modes when measuring each ratio of branching fractions and $\Gamma_{\pm\pm}/\Gamma$. It is conservatively estimated using the data-driven MC corrections for dimuon triggers, applying them to all reconstructed events and taking the deviation from the nominal result. The effect amounts to 0.6% for $R_{D_s^{(*)+}/\pi^+}$. For $R_{D_s^{*+}/D_s^+}$ and $\Gamma_{\pm\pm}/\Gamma$ it is estimated at the level below 0.2% and neglected. The fraction of signal decay events with muons not matching those which fire the triggers is found to be about 1.5% and does not affect the measured quantities.

- The muon reconstruction and identification efficiency uncertainty affects the individual channel efficiencies by about 1%–2%. However, these mostly cancel out in the efficiency ratios and the effect is found to be below 0.1% for the measured quantities and is neglected.

- The presence of *other D_s^+ decay modes* with a $K^+K^-\pi^+$ final state affects the selection efficiency. This is studied with a dedicated MC simulation. The dominant contribution is found to come from $D_s^+ \to f_0(980)(K^+K^-)\pi^+$ decay, due to the large overlap of its $m(K^+K^-)$ distribution with the signal one. By considering a range of possible values for the mass and natural width of the $f_0(980)$ meson [25] to quantify that overlap, an uncertainty of 1.6% is assigned to the $R_{D_s^{(*)+}/\pi^+}$ ratios.

The following variations are used to estimate uncertainties due to the $B_c^+ \to J/\psi D_s^{(*)+}$ signal fit procedure.

- $B_c^+ \to J/\psi D_s^+$ *signal mass shape modelling* effects are tested with alternative models for the $B_c^+ \to J/\psi D_s^+$ signal $m(J/\psi D_s^+)$ distribution: a double-Gaussian function and a double-sided Crystal Ball function [34–36], fixing the tail parameters to the values extracted from simulation. Changes in the $B_c^+ \to J/\psi D_s^+$ yield are found to be less than 1.8%, with smaller effects on $B_c^+ \to J/\psi D_s^{*+}$ and $f_{\pm\pm}$.

- For the $B_c^+ \to J/\psi D_s^{*+}$ *signal mass shape*, variations of the bandwidth scale factor in the kernel templates (ρ parameter defined in ref. [29]) in the widest range preserving both smoothness and a sufficient level of detail in the distributions are applied. The $m(J/\psi D_s^+)$ resolution is also varied by $\pm 10\%$. The largest effect found is 2.7%, for the $f_{\pm\pm}$ value.

- The simulated *shapes of the $|\cos\theta'(\mu^+)|$ templates for $B_c^+ \to J/\psi D_s^{(*)+}$ signals* are varied by similar changes of the kernel bandwidth scale factor parameter. The effect on all measured quantities is below 0.6%.

- For the *background mass shape modelling*, the two-parameter exponential function and a second-order polynomial function are used as alternatives to the simple exponential shape; the fitted mass range is also reduced in turn by 40 MeV (two bins of the mass distributions in figure 2) from the low-mass and high-mass ends. These variations represent the largest uncertainty in the $B_c^+ \to J/\psi D_s^{(*)+}$ signal extraction and amount to 6.0%, 9.0%, and 3.2% for $R_{D_s^+/\pi^+}$, $R_{D_s^{*+}/\pi^+}$, and $R_{D_s^{*+}/D_s^+}$, respectively.

- The *background $|\cos\theta'(\mu^+)|$ shape* is alternatively parameterized with a third-order polynomial function. A linear combination of the kernel templates made from the left and right data sidebands is also used to describe the background in the mass range of the signals. The latter variation also covers a small deviation from the assumption of factorization of the mass and angular parts of the background PDF. These variations yield a maximum change of about 2% for $R_{D_s^{*+}/D_s^+}$ and $\Gamma_{\pm\pm}/\Gamma$, and about 1% for $R_{D_s^+/\pi^+}$ and $R_{D_s^{*+}/\pi^+}$.

- Effect of the $B_s^0 \to \mu^+\mu^-\phi$ *triggers*: in the nominal fit, the angular and mass shapes of the signals are supposed to be the same in Datasets 1 and 2, and the same value of $f_{\pm\pm}$ is used in both. To estimate the possible effects of deviations from these assumptions, alternative fit models with either of the following changes are tested:
  - different signal mass and $|\cos\theta'(\mu^+)|$ templates are used for Datasets 1 and 2 (produced from events selected by the corresponding triggers);
  - the $f_{\pm\pm}$ fraction is set to be different between Datasets 1 and 2 according to slightly different efficiencies in the simulation.

  These variations yield an uncertainty of about 4% for $\Gamma_{\pm\pm}/\Gamma$ and less than 1.5% for the R ratios.

- The *branching fractions of the D_s^{*+} decays* are varied in simulation within their uncertainties [25] since they affect the $B_c^+ \to J/\psi D_s^{*+}$ template shapes. The effect is found to be 0.7% for $\Gamma_{\pm\pm}/\Gamma$ and below 0.1% for the other quantities.

The following variations are used to estimate uncertainties due to the $B_c^+ \to J/\psi\pi^+$ signal fit procedure.

- For the *signal modelling*, a double-Gaussian function and a double-sided Crystal Ball function are used as alternatives to the modified Gaussian function, eq. (4.1), fixing the tail parameters to the values extracted from simulation. Changes in the signal yields reach 4.2%.

- Alternative models are used for *combinatorial background modelling*: a three-parameter exponential function, and second- and third-order polynomial functions are used. These models, providing more freedom at lower $m(J/\psi\pi^+)$ values, are able to absorb a part of PRD contribution that may not have been accounted for by using the $B_c^+ \to J/\psi\rho^+$ templates. Alternatively, an additional hyperbolic tangent function is added to the fit PDF to cover possible mis-modelling of the PRD component. The shape of the $B_c^+ \to J/\psi\rho^+$ templates is also varied by changing the kernel bandwidth scale factor and $m(J/\psi\pi^+)$ resolution. These variations produced changes of up to 5.8% in the signal yield.

- For the *CKM-suppressed peaking background* from $B_c^+ \to J/\psi K^+$, its fraction is varied according to the uncertainty in the measured value of $\mathcal{B}(B_c^+ \to J/\psi K^+)/\mathcal{B}(B_c^+ \to J/\psi\pi^+)$ [25]. The change in the signal yield is 1%.

The statistical uncertainties of the total efficiency values due to the limited number of MC events are also treated as a separate source of systematic uncertainty.

Contributions from the different sources of systematic uncertainty described above are summed in quadrature. Finally, since the branching fraction of $D_s^+ \to \phi(K^+K^-)\pi^+$ is featured in eq. (5.1), its uncertainty [32] is propagated to the final values of the relative branching fractions $R_{D_s^{(*)+}/\pi^+}$. This uncertainty is quoted separately.

The systematic uncertainties of the measured quantities are summarized in table 4.

7 Results and discussion

The ratios of the branching fractions for $B_c^+ \to J/\psi D_s^{(*)+}$ and $B_c^+ \to J/\psi\pi^+$ calculated according to eq. (5.1) are found to be

$$R_{D_s^+/\pi^+} = 2.76 \pm 0.33 \pm 0.29 \pm 0.16$$

and

$$R_{D_s^{*+}/\pi^+} = 5.33 \pm 0.61 \pm 0.67 \pm 0.32,$$

where the first uncertainty is statistical, the second is systematic, and the third corresponds to the uncertainty in the branching fraction of the $D_s^+ \to \phi(K^+K^-)\pi^+$ decay. The ratio of the branching fractions for $B_c^+ \to J/\psi D_s^{*+}$ and $B_c^+ \to J/\psi D_s^+$ calculated according to eq. (5.2) is found to be

$$R_{D_s^{*+}/D_s^+} = 1.93 \pm 0.24 \pm 0.09.$$

Source	Uncertainty [%]			
	$R_{D_s^+/\pi^+}$	$R_{D_s^{*+}/\pi^+}$	$R_{D_s^{*+}/D_s^+}$	$\Gamma_{\pm\pm}/\Gamma$
Simulated $p_{\mathrm{T}}(B_c^+)$ spectrum	1.5	1.9	0.4	0.1
Simulated $|\eta(B_c^+)|$ spectrum	0.7	0.7	0.1	0.2
B_c^+ lifetime	0.1	< 0.1	—	—
D_s^+ lifetime	0.4	0.4	—	—
Tracking efficiency	1.0	1.0	< 0.1	< 0.1
Pile-up effects	1.0	1.0	—	—
χ^2/N_{dof} selection efficiency	3.2	3.2	—	—
Impact parameter selection efficiency	0.2	0.2	—	—
BDT selection efficiency	1.3	1.3	—	—
Trigger efficiency	0.6	0.6	—	—
Other D_s^+ decay modes	1.6	1.6	—	—
$B_c^+ \to J/\psi D_s^{(*)+}$ signal fit:				
D_s^+ signal mass modelling	1.8	0.5	1.3	0.8
D_s^{*+} signal mass modelling	0.6	1.2	1.7	2.7
Signal angular modelling	0.4	< 0.1	0.4	0.6
Background mass modelling	6.0	9.0	3.2	1.0
Background angular modelling	0.9	1.3	2.1	2.4
$B_s^0 \to \mu^+\mu^-\phi$ triggers	0.8	0.5	1.3	4.0
D_s^{*+} branching fractions	< 0.1	< 0.1	< 0.1	0.7
$B_c^+ \to J/\psi\pi^+$ signal fit:				
Signal modelling	4.2	4.2	—	—
PRD/comb. background modelling	5.8	5.8	—	—
CKM-suppr. background modelling	1.0	1.0	—	—
MC statistics	1.5	1.5	1.7	1.5
Total	10.7	12.6	4.9	5.8
$\mathcal{B}(D_s^+ \to \phi(K^+K^-)\pi^+)$	5.9	5.9	—	—

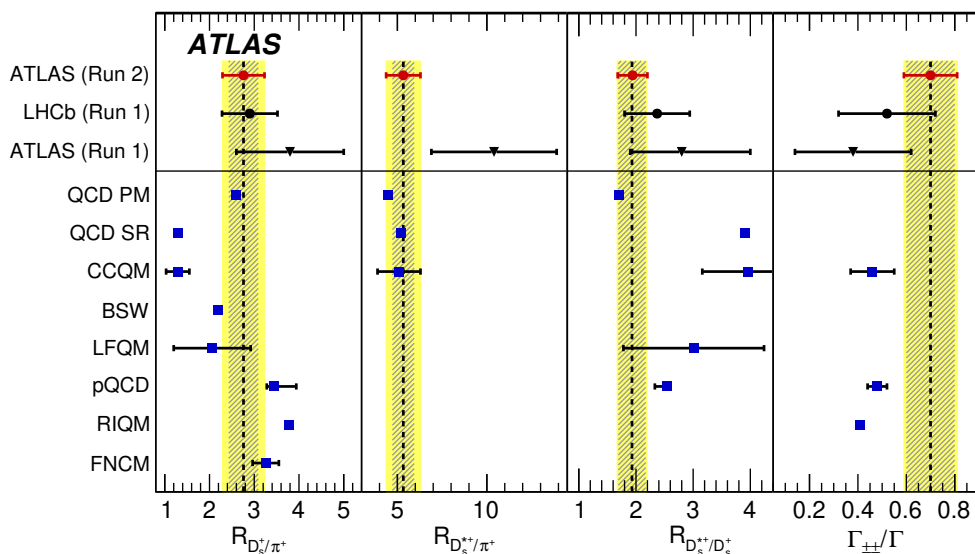**Table 4**. Relative systematic uncertainties of the measured quantities.

Figure 4. Comparison of the results of this measurement with those of ATLAS Run 1 [2], LHCb [1] and theoretical predictions based on a QCD relativistic potential model (QCD PM) [3], QCD sum rules (QCD SR) [4], covariant confined quark model (CCQM) [6], Bauer-Stech-Wirbel relativistic quark model (BSW) [7], light-front quark model (LFQM) [8], perturbative QCD (pQCD) [9], relativistic independent quark model (RIQM) [10, 11], and calculations in the QCD factorization approach (FNCM) [12]. Hatched areas show the statistical uncertainties of this measurement and yellow bands correspond to the total uncertainties. Quadrature sums of all experimental uncertainties are quoted for the ATLAS Run 1 and LHCb results. The uncertainties of the theoretical predictions are shown only if they are explicitly quoted in the corresponding papers.

The fraction of transverse polarization in $B_c^+ \to J/\psi D_s^{*+}$ decay calculated according to eq. (5.3) is found to be

$$\Gamma_{\pm\pm}/\Gamma = 0.70 \pm 0.10 \pm 0.04.$$

In the last two quantities, the first uncertainty is statistical and the second is systematic.

These ATLAS results from Run 2 are compared with the results of LHCb [1] and ATLAS Run 1 [2] measurements and with the predictions from various theoretical calculations in table 5 and figure 4. The measurements of $R_{D_s^+/\pi^+}$ and $R_{D_s^{*+}/D_s^+}$ agree with the ATLAS Run 1 and LHCb results. The obtained values of $R_{D_s^{*+}/\pi^+}$ and $\Gamma_{\pm\pm}/\Gamma$ are, respectively, smaller and larger than in the ATLAS Run 1 measurement, although in each case the difference does not exceed 1.5 standard deviations of the Run 1 uncertainty. Since the precision of the new results significantly exceeds that achieved in the ATLAS Run 1 analysis [2], the latter is superseded by this work.

The ratios of branching fractions are well described by the predictions of a QCD relativistic potential model [3]. The predictions of a QCD sum rules calculation [4], the covariant confined quark model [6][4] and the light-front quark model [8] all underestimate

---

[4]The predictions of relativistic quark model [5] are made within a very similar approach, so only the updated result from ref. [6] is discussed.

$R_{D_s^+/\pi^+}$	$R_{D_s^{*+}/\pi^+}$	$R_{D_s^{*+}/D_s^+}$	$\Gamma_{\pm\pm}/\Gamma$	Reference
2.76 ± 0.47	5.33 ± 0.96	1.93 ± 0.26	0.70 ± 0.11	ATLAS Run 2
2.90 ± 0.62	—	2.37 ± 0.57	0.52 ± 0.20	LHCb Run 1 [1]
3.8 ± 1.2	10.4 ± 3.5	$2.8^{+1.2}_{-0.9}$	0.38 ± 0.24	ATLAS Run 1 [2]
2.6	4.5	1.7	—	QCD potential model [3]
1.3	5.2	3.9	—	QCD sum rules [4]
1.29 ± 0.26	5.09 ± 1.02	3.96 ± 0.80	0.46 ± 0.09	CCQM [6]
2.2	—	—	—	BSW [7]
2.06 ± 0.86	—	3.01 ± 1.23	—	LFQM [8]
$3.45^{+0.49}_{-0.17}$	—	$2.54^{+0.07}_{-0.21}$	0.48 ± 0.04	pQCD [9]
3.7832	—	—	0.410	RIQM [10, 11]
3.257 ± 0.293	—	—	—	FNCM [12]
1.67 ± 0.36	3.49 ± 0.52	2.09 ± 0.52	—	$B^+ \to \bar{D}^{*0}D_s^{(*)+}/\bar{D}^{*0}\pi^+$ [25]
2.92 ± 0.42	6.46 ± 0.60	2.21 ± 0.35	0.48 ± 0.05	$B^0 \to D^{*-}D_s^{(*)+}/D^{*-}\pi^+$ [25]
—	7.2 ± 2.1	—	0.94 ± 0.18	$B_s^0 \to D_s^{*-}D_s^+/D_s^{*-}\pi^+$ [25]
—	—	1.402 ± 0.083	0.396 ± 0.023	$B^+ \to J/\psi K^{(*)+}$ [25]
—	—	1.425 ± 0.065	0.429 ± 0.007	$B^0 \to J/\psi K^{(*)0}$ [25]
—	—	—	0.4774 ± 0.0034	$B_s^0 \to J/\psi\phi$ [25]

Table 5. Comparison of the measured quantities with the results of earlier measurements and theory predictions. Values of the corresponding ratios of branching fractions calculated using eqs. (7.1)–(7.3) and eq. (7.4) and of transverse polarization fractions for B^+, B^0, and B_s^0 decays are also shown. No phase-space corrections are applied to the ratios and the quoted uncertainties are the ones propagated from the world average uncertainties of the individual decay branching fractions. For all experimental measurements, quadrature sums of all uncertainties are quoted. Uncertainties in the predictions are quoted only if they are explicitly given in the corresponding references.

the $R_{D_s^+/\pi^+}$ ratio, although the prediction of the latter model still agrees with data within a large theoretical uncertainty. However, the $R_{D_s^{*+}/\pi^+}$ ratio is described well by the same predictions, which correspondingly overestimate the $R_{D_s^{*+}/D_s^+}$ ratio. Nonetheless, for the light-front quark model the predicted value of $R_{D_s^{*+}/D_s^+}$ is still in agreement within the theoretical uncertainty.

The $R_{D_s^+/\pi^+}$ value predicted in the Bauer-Stech-Wirbel framework [7] is slightly below the data, while the results of calculations within perturbative QCD [9] and the QCD factorization approach [12] are near the upper bound of the experimental uncertainty range; the recent prediction made within the framework of the relativistic independent quark model [11] gives an even higher value. The perturbative QCD prediction [9] for the $R_{D_s^{*+}/D_s^+}$ ratio is also slightly above the data.

The measured value of $\Gamma_{\pm\pm}/\Gamma$ clearly agrees with a naive spin-counting expectation of 2/3. It is larger than the values calculated in the covariant confined quark model [6], perturbative QCD [9], and the relativistic independent quark model [10], which give values below 0.5. The discrepancies, however, do not exceed 2–3 standard deviations of the experimental uncertainty.

The measured ratios of branching fractions and the transverse polarization fraction can be compared with the corresponding quantities for the other B mesons. Assuming that the colour-favoured spectator diagram (shown in figure 1(a) for $B_c^+ \to J/\psi D_s^{(*)+}$) dominates the decay amplitudes, the following approximate relations can be established:

$$R_{D_s^+/\pi^+} \approx \frac{\Gamma(B \to \bar{D}^* D_s^+)}{\Gamma(B \to \bar{D}^* \pi^+)}, \tag{7.1}$$

$$R_{D_s^{*+}/\pi^+} \approx \frac{\Gamma(B \to \bar{D}^* D_s^{*+})}{\Gamma(B \to \bar{D}^* \pi^+)}, \tag{7.2}$$

$$R_{D_s^{*+}/D_s^+} \approx \frac{\Gamma(B \to \bar{D}^* D_s^{*+})}{\Gamma(B \to \bar{D}^* D_s^+)}, \tag{7.3}$$

where B and $\bar{D}^*$ stand for B^+ and $\bar{D}^{*0}$, B^0 and D^{*-}, or B_s^0 and D_s^{*-}. Similarly, the $\Gamma_{\pm\pm}/\Gamma$ value for $B_c^+ \to J/\psi D_s^{*+}$ decay can be compared with the same quantity in the corresponding B^+ or B_s^0 decays.

One can also compare the measured value of $R_{D_s^{*+}/D_s^+}$ with the corresponding ratio for the B^0 and B^+ decays occurring predominantly via the colour-suppressed spectator diagram:

$$R_{D_s^{*+}/D_s^+} \sim \frac{\Gamma(B \to J/\psi K^*)}{\Gamma(B \to J/\psi K)}, \tag{7.4}$$

where B stands for B^+ or B^0 and $K^{(*)}$ is $K^{(*)+}$ or $K^{(*)0}$, respectively. The $\Gamma_{\pm\pm}/\Gamma$ value, in turn, can be compared with the transverse polarization fraction in the same $B \to J/\psi K^*$ decays as well as in $B_s^0 \to J/\psi \phi$ decays.

The estimates obtained using eqs. (7.1)–(7.3) and eq. (7.4) with the world average branching fraction values for the B^0, B^+, and B_s^0 decays [25] are also shown in table 5, along with the $\Gamma_{\pm\pm}/\Gamma$ values for the corresponding decays of those mesons [25]. Corrections to the above approximations, required due to phase-space differences between the studied B_c decays and the corresponding B^+, B^0, and B_s^0 decays, are 1%–2% for eqs. (7.1)–(7.3) and increase the values from eq. (7.4) by about 7%. These corrections are not applied in the numbers quoted in table 5.

The $R_{D_s^{*+}/D_s^+}$ value agrees with the corresponding ratio calculated with eq. (7.3) for both the B^0 and B^+ decays and is larger than that obtained from eq. (7.4) for decays of the same mesons. It supports the assumption that the colour-favoured spectator diagram dominates the $B_c^+ \to J/\psi D_s^{(*)+}$ decay amplitudes. The $R_{D_s^+/\pi^+}$ and $R_{D_s^{*+}/\pi^+}$ values agree with the calculations made using eqs. (7.1)–(7.2) for decays of B^0 and B_s^0, and are larger than those for decays of B^+. The measured value of $\Gamma_{\pm\pm}/\Gamma$ lies between the transverse polarization fraction values in the $B^0 \to D^{*-} D_s^*$ and $B_s^0 \to D_s^{*-} D_s^*$ decays and is larger than one in the considered B decays occurring via the colour-suppressed spectator diagram.

8   Summary

A study of $B_c^+ \to J/\psi D_s^+$ and $B_c^+ \to J/\psi D_s^{*+}$ decays has been performed by the ATLAS experiment at the LHC using *pp* collision data corresponding to an integrated luminosity of $139\,\text{fb}^{-1}$ at $13\,\text{TeV}$ centre-of-mass energy. The ratios of the branching fractions of these decays to the branching fraction of $B_c^+ \to J/\psi \pi^+$ decay are measured to be $R_{D_s^+/\pi^+} = 2.76 \pm 0.33 \pm 0.29 \pm 0.16$ and $R_{D_s^{*+}/\pi^+} = 5.33 \pm 0.61 \pm 0.67 \pm 0.32$, where the first uncertainty is statistical, the second is systematic, and the third is due to the uncertainty in the branching fraction of $D_s^+ \to \phi(K^+K^-)\pi^+$ decay. The ratio of the two decay branching fractions is also measured, yielding $R_{D_s^{*+}/D_s^+} = 1.93 \pm 0.24 \pm 0.09$. The transverse polarization fraction in the $B_c^+ \to J/\psi D_s^{*+}$ decay is found to be $\Gamma_{\pm\pm}/\Gamma = 0.70 \pm 0.10 \pm 0.04$. The results of this new measurement supersede those of the previous ATLAS measurement using Run 1 data.

All results are consistent with the earlier measurements by ATLAS and LHCb. The precision of the measurement exceeds that of all previous studies of these decays.

Various predictions for the measured quantities are compared with data. A QCD relativistic potential model calculation agrees well with all three ratios of branching fractions. The $R_{D_s^{*+}/\pi^+}$ ratio also agrees with other calculations made using QCD sum rules and the covariant confined quark model. The $R_{D_s^+/\pi^+}$ and $R_{D_s^{*+}/D_s^+}$ ratios are, however, poorly described by the same predictions. The measured transverse polarization fraction in the $B_c^+ \to J/\psi D_s^{*+}$ decay agrees well with the value of 2/3 expected from naive spin-counting considerations, while the available calculations of this quantity in the covariant confined quark model, perturbative QCD, and the relativistic independent quark model give values below the data, although agreeing within 2–3 standard deviations of experimental uncertainty.

Comparisons of the measured $R_{D_s^{*+}/D_s^+}$ ratio with the similar ratios for the B^0 and B^+ meson decays support the assumption that the colour-favoured spectator diagram dominates the $B_c^+ \to J/\psi D_s^{(*)+}$ decay amplitudes.

References

[1] LHCb collaboration, *Observation of $B_c^+ \to J/\psi D_s^+$ and $B_c^+ \to J/\psi D_s^{*+}$ decays*, *Phys. Rev. D* **87** (2013) 112012 [*Addendum ibid.* **89** (2014) 019901] [arXiv:1304.4530] [INSPIRE].

[2] ATLAS collaboration, *Study of the $B_c^+ \to J/\psi D_s^+$ and $B_c^+ \to J/\psi D_s^{*+}$ decays with the ATLAS detector*, *Eur. Phys. J. C* **76** (2016) 4 [arXiv:1507.07099] [INSPIRE].

[3] P. Colangelo and F. De Fazio, *Using heavy quark spin symmetry in semileptonic B_c decays*, *Phys. Rev. D* **61** (2000) 034012 [hep-ph/9909423] [INSPIRE].

[4] V.V. Kiselev, *Exclusive decays and lifetime of B_c meson in QCD sum rules*, hep-ph/0211021 [INSPIRE].

[5] M.A. Ivanov, J.G. Korner and P. Santorelli, *Exclusive semileptonic and nonleptonic decays of the B_c meson*, *Phys. Rev. D* **73** (2006) 054024 [hep-ph/0602050] [INSPIRE].

[6] S. Dubnicka, A.Z. Dubnickova, A. Issadykov, M.A. Ivanov and A. Liptaj, *Study of B_c decays into charmonia and D mesons*, *Phys. Rev. D* **96** (2017) 076017 [arXiv:1708.09607] [INSPIRE].

[7] R. Dhir and R.C. Verma, *B_c Meson Form-factors and $B_c \to PV$ Decays Involving Flavor Dependence of Transverse Quark Momentum*, *Phys. Rev. D* **79** (2009) 034004 [arXiv:0810.4284] [INSPIRE].

[8] H.-W. Ke, T. Liu and X.-Q. Li, *Transitions of $B_c \to \psi(1S, 2S)$ and the modified harmonic oscillator wave function in LFQM*, *Phys. Rev. D* **89** (2014) 017501 [arXiv:1307.5925] [INSPIRE].

[9] Z. Rui and Z.-T. Zou, *S-wave ground state charmonium decays of B_c mesons in the perturbative QCD approach*, *Phys. Rev. D* **90** (2014) 114030 [`arXiv:1407.5550`] [INSPIRE].

[10] S. Kar, P.C. Dash, M. Priyadarsini, S. Naimuddin and N. Barik, *Nonleptonic $B_c \to VV$ decays*, *Phys. Rev. D* **88** (2013) 094014 [INSPIRE].

[11] L. Nayak, P.C. Dash, S. Kar and N. Barik, *Exclusive nonleptonic B_c-meson decays to S-wave charmonium states*, *Phys. Rev. D* **105** (2022) 053007 [`arXiv:2202.01167`] [INSPIRE].

[12] B. Mohammadi, *The branching fraction calculations of $B_c^+ \to \psi(2S)\pi^+, B_c^+ \to J/\psi K^+$ and $B_c^+ \to J/\psi D_s^+$ decays relative to that of the $B_c^+ \to J/\psi\pi^+$ mode*, *Int. J. Mod. Phys. A* **33** (2018) 1850044 [*Erratum ibid.* **33** (2018) 1892003] [INSPIRE].

[13] ATLAS collaboration, *The ATLAS Experiment at the CERN Large Hadron Collider*, 2008 *JINST* **3** S08003 [INSPIRE].

[14] ATLAS IBL collaboration, *Production and Integration of the ATLAS Insertable B-Layer*, 2018 *JINST* **13** T05008 [`arXiv:1803.00844`] [INSPIRE].

[15] ATLAS collaboration, *ATLAS data quality operations and performance for 2015–2018 data-taking*, 2020 *JINST* **15** P04003 [`arXiv:1911.04632`] [INSPIRE].

[16] ATLAS collaboration, *Luminosity determination in pp collisions at $\sqrt{s} = 13\,TeV$ using the ATLAS detector at the LHC*, ATLAS-CONF-2019-021 (2019).

[17] G. Avoni et al., *The new LUCID-2 detector for luminosity measurement and monitoring in ATLAS*, 2018 *JINST* **13** P07017 [INSPIRE].

[18] C.-H. Chang, X.-Y. Wang and X.-G. Wu, *BCVEGPY2.2: A newly upgraded version for hadronic production of the meson Bc and its excited states*, *Comput. Phys. Commun.* **197** (2015) 335 [`arXiv:1507.05176`] [INSPIRE].

[19] T. Sjöstrand et al., *An introduction to PYTHIA 8.2*, *Comput. Phys. Commun.* **191** (2015) 159 [`arXiv:1410.3012`] [INSPIRE].

[20] D.J. Lange, *The EvtGen particle decay simulation package*, *Nucl. Instrum. Meth. A* **462** (2001) 152 [INSPIRE].

[21] ATLAS collaboration, *The ATLAS Simulation Infrastructure*, *Eur. Phys. J. C* **70** (2010) 823 [`arXiv:1005.4568`] [INSPIRE].

[22] GEANT4 collaboration, *GEANT4 — a simulation toolkit*, *Nucl. Instrum. Meth. A* **506** (2003) 250 [INSPIRE].

[23] ATLAS collaboration, *The ATLAS collaboration Software and Firmware*, ATL-SOFT-PUB-2021-001 (2021).

[24] ATLAS collaboration, *Muon reconstruction and identification efficiency in ATLAS using the full Run 2 pp collision data set at $\sqrt{s} = 13\,TeV$*, *Eur. Phys. J. C* **81** (2021) 578 [`arXiv:2012.00578`] [INSPIRE].

[25] PARTICLE DATA collaboration, *Review of Particle Physics*, *Prog. Theor. Exp. Phys.* **2020** (2020) 083C01 [INSPIRE].

[26] V. Kostyukhin, *VKalVrt — package for vertex reconstruction in ATLAS*, ATL-PHYS-2003-031 (2003).

[27] A. Hocker et al., *TMVA — Toolkit for Multivariate Data Analysis*, `physics/0703039` [INSPIRE].

[28] ATLAS collaboration, *Performance of the ATLAS muon triggers in Run 2*, 2020 *JINST* **15** P09015 [`arXiv:2004.13447`] [INSPIRE].

[29] K. Cranmer, *Kernel estimation in high-energy physics*, *Comput. Phys. Commun.* **136** (2001) 198 [`hep-ex/0011057`] [INSPIRE].

[30] ZEUS collaboration, *Measurement of inelastic J/ψ production in deep inelastic scattering at HERA*, *Eur. Phys. J. C* **44** (2005) 13 [`hep-ex/0505008`] [INSPIRE].

[31] ATLAS collaboration, *Measurement of the b-hadron production cross section using decays to $D^{*+}\mu^-X$ final states in pp collisions at $\sqrt{s} = 7$ TeV with the ATLAS detector*, *Nucl. Phys. B* **864** (2012) 341 [`arXiv:1206.3122`] [INSPIRE].

[32] CLEO collaboration, *Absolute Measurement of Hadronic Branching Fractions of the D_s^+ Meson*, *Phys. Rev. Lett.* **100** (2008) 161804 [`arXiv:0801.0680`] [INSPIRE].

[33] M. Pivk and F.R. Le Diberder, *SPlot: A Statistical tool to unfold data distributions*, *Nucl. Instrum. Meth. A* **555** (2005) 356 [`physics/0402083`] [INSPIRE].

[34] M. Oreglia, *A Study of the Reactions $\psi' \to \gamma\gamma\psi$*, Ph.D. Thesis, Stanford University, Stanford, CA, U.S.A. (1980) [SLAC-R-236] and online at http://www.slac.stanford.edu/pubs/slacreports/slac-r-236.html.

[35] J. Gaiser, *Charmonium Spectroscopy From Radiative Decays of the J/ψ and ψ'*, Ph.D. Thesis, Stanford University, Stanford, CA, U.S.A. (1982) [SLAC-R-255] and online at https://www-public.slac.stanford.edu/sciDoc/docMeta.aspx?slacPubNumber=slac-r-255.

[36] T. Skwarnicki, *A study of the radiative cascade transitions between the Υ' and Υ resonances*, Ph.D. Thesis, Cracow Institute of Nuclear Physics, Cracow, Poland (1986) [DESY-F31-86-02] [INSPIRE].

[37] ATLAS collaboration, *ATLAS Computing Acknowledgements*, ATL-SOFT-PUB-2021-003 (2021).

The ATLAS collaboration

G. Aad[98], B. Abbott[124], D.C. Abbott[99], A. Abed Abud[34], K. Abeling[51], D.K. Abhayasinghe[91],
S.H. Abidi[27], A. Aboulhorma[33e], H. Abramowicz[157], H. Abreu[156], Y. Abulaiti[5],
A.C. Abusleme Hoffman[142a], B.S. Acharya[64a,64b,o], B. Achkar[51], L. Adam[96],
C. Adam Bourdarios[4], L. Adamczyk[81a], L. Adamek[162], S.V. Addepalli[24], J. Adelman[116],
A. Adiguzel[11c,ac], S. Adorni[52], T. Adye[139], A.A. Affolder[141], Y. Afik[34], C. Agapopoulou[62],
M.N. Agaras[12], J. Agarwala[68a,68b], A. Aggarwal[114], C. Agheorghiesei[25c],
J.A. Aguilar-Saavedra[135f,135a,ab], A. Ahmad[34], F. Ahmadov[77,z], W.S. Ahmed[100], X. Ai[44],
G. Aielli[71a,71b], I. Aizenberg[175], S. Akatsuka[83], M. Akbiyik[96], T.P.A. Åkesson[94],
A.V. Akimov[107], K. Al Khoury[37], G.L. Alberghi[21b], J. Albert[171], P. Albicocco[49],
M.J. Alconada Verzini[86], S. Alderweireldt[48], M. Aleksa[34], I.N. Aleksandrov[77], C. Alexa[25b],
T. Alexopoulos[9], A. Alfonsi[115], F. Alfonsi[21b], M. Alhroob[124], B. Ali[137], S. Ali[154], M. Aliev[161],
G. Alimonti[66a], C. Allaire[34], B.M.M. Allbrooke[152], P.P. Allport[19], A. Aloisio[67a,67b], F. Alonso[86],
C. Alpigiani[144], E. Alunno Camelia[71a,71b], M. Alvarez Estevez[95], M.G. Alviggi[67a,67b],
Y. Amaral Coutinho[78b], A. Ambler[100], L. Ambroz[130], C. Amelung[34], D. Amidei[102],
S.P. Amor Dos Santos[135a], S. Amoroso[44], K.R. Amos[169], C.S. Amrouche[52], V. Ananiev[129],
C. Anastopoulos[145], N. Andari[140], T. Andeen[10], J.K. Anders[18], S.Y. Andrean[43a,43b],
A. Andreazza[66a,66b], S. Angelidakis[8], A. Angerami[37], A.V. Anisenkov[117b,117a], A. Annovi[69a],
C. Antel[52], M.T. Anthony[145], E. Antipov[125], M. Antonelli[49], D.J.A. Antrim[16], F. Anulli[70a],
M. Aoki[79], J.A. Aparisi Pozo[169], M.A. Aparo[152], L. Aperio Bella[44], N. Aranzabal[34],
V. Araujo Ferraz[78a], C. Arcangeletti[49], A.T.H. Arce[47], E. Arena[88], J-F. Arguin[106],
S. Argyropoulos[50], J.-H. Arling[44], A.J. Armbruster[34], A. Armstrong[166], O. Arnaez[162],
H. Arnold[34], Z.P. Arrubarrena Tame[110], G. Artoni[130], H. Asada[112], K. Asai[122], S. Asai[159],
N.A. Asbah[57], E.M. Asimakopoulou[167], L. Asquith[152], J. Assahsah[33d], K. Assamagan[27],
R. Astalos[26a], R.J. Atkin[31a], M. Atkinson[168], N.B. Atlay[17], H. Atmani[58b], P.A. Atmasiddha[102],
K. Augsten[137], S. Auricchio[67a,67b], V.A. Austrup[177], G. Avner[156], G. Avolio[34], M.K. Ayoub[13c],
G. Azuelos[106,aj], D. Babal[26a], H. Bachacou[140], K. Bachas[158], A. Bachiu[32], F. Backman[43a,43b],
A. Badea[57], P. Bagnaia[70a,70b], H. Bahrasemani[148], A.J. Bailey[169], V.R. Bailey[168],
J.T. Baines[139], C. Bakalis[9], O.K. Baker[178], P.J. Bakker[115], E. Bakos[14], D. Bakshi Gupta[7],
S. Balaji[153], R. Balasubramanian[115], E.M. Baldin[117b,117a], P. Balek[138], E. Ballabene[66a,66b],
F. Balli[140], L.M. Baltes[59a], W.K. Balunas[130], J. Balz[96], E. Banas[82], M. Bandieramonte[134],
A. Bandyopadhyay[22], S. Bansal[22], L. Barak[157], E.L. Barberio[101], D. Barberis[53b,53a],
M. Barbero[98], G. Barbour[92], K.N. Barends[31a], T. Barillari[111], M-S. Barisits[34], J. Barkeloo[127],
T. Barklow[149], B.M. Barnett[139], R.M. Barnett[16], A. Baroncelli[58a], G. Barone[27], A.J. Barr[130],
L. Barranco Navarro[43a,43b], F. Barreiro[95], J. Barreiro Guimarães da Costa[13a], U. Barron[157],
S. Barsov[133], F. Bartels[59a], R. Bartoldus[149], G. Bartolini[98], A.E. Barton[87], P. Bartos[26a],
A. Basalaev[44], A. Basan[96], M. Baselga[44], I. Bashta[72a,72b], A. Bassalat[62,ag], M.J. Basso[162],
C.R. Basson[97], R.L. Bates[55], S. Batlamous[33e], J.R. Batley[30], B. Batool[147], M. Battaglia[141],
M. Bauce[70a,70b], F. Bauer[140,*], P. Bauer[22], H.S. Bawa[29], A. Bayirli[11c], J.B. Beacham[47],
T. Beau[131], P.H. Beauchemin[165], F. Becherer[50], P. Bechtle[22], H.P. Beck[18,q], K. Becker[173],
C. Becot[44], A.J. Beddall[11a], V.A. Bednyakov[77], C.P. Bee[151], T.A. Beermann[34], M. Begalli[78b],
M. Begel[27], A. Behera[151], J.K. Behr[44], C. Beirao Da Cruz E Silva[34], J.F. Beirer[51,34],
F. Beisiegel[22], M. Belfkir[4], G. Bella[157], L. Bellagamba[21b], A. Bellerive[32], P. Bellos[19],
K. Beloborodov[117b,117a], K. Belotskiy[108], N.L. Belyaev[108], D. Benchekroun[33a],
Y. Benhammou[157], D.P. Benjamin[27], M. Benoit[27], J.R. Bensinger[24], S. Bentvelsen[115],
L. Beresford[34], M. Beretta[49], D. Berge[17], E. Bergeaas Kuutmann[167], N. Berger[4],
B. Bergmann[137], L.J. Bergsten[24], J. Beringer[16], S. Berlendis[6], G. Bernardi[131], C. Bernius[149],
F.U. Bernlochner[22], T. Berry[91], P. Berta[138], A. Berthold[46], I.A. Bertram[87],

O. Bessidskaia Bylund[177], S. Bethke[111], A. Betti[40], A.J. Bevan[90], S. Bhatta[151],
D.S. Bhattacharya[172], P. Bhattarai[24], V.S. Bhopatkar[5], R. Bi[134], R.M. Bianchi[134], O. Biebel[110],
R. Bielski[127], N.V. Biesuz[69a,69b], M. Biglietti[72a], T.R.V. Billoud[137], M. Bindi[51], A. Bingul[11d],
C. Bini[70a,70b], S. Biondi[21b,21a], A. Biondini[88], C.J. Birch-sykes[97], G.A. Bird[19,139], M. Birman[175],
T. Bisanz[34], J.P. Biswal[2], D. Biswas[176,j], A. Bitadze[97], C. Bittrich[46], K. Bjørke[129], I. Bloch[44],
C. Blocker[24], A. Blue[55], U. Blumenschein[90], J. Blumenthal[96], G.J. Bobbink[115],
V.S. Bobrovnikov[117b,117a], M. Boehler[50], D. Bogavac[12], A.G. Bogdanchikov[117b,117a], C. Bohm[43a],
V. Boisvert[91], P. Bokan[44], T. Bold[81a], M. Bomben[131], M. Bona[90], M. Boonekamp[140],
C.D. Booth[91], A.G. Borbély[55], H.M. Borecka-Bielska[106], L.S. Borgna[92], G. Borissov[87],
D. Bortoletto[130], D. Boscherini[21b], M. Bosman[12], J.D. Bossio Sola[34], K. Bouaouda[33a],
J. Boudreau[134], E.V. Bouhova-Thacker[87], D. Boumediene[36], R. Bouquet[131], A. Boveia[123],
J. Boyd[34], D. Boye[27], I.R. Boyko[77], A.J. Bozson[91], J. Bracinik[19], N. Brahimi[58d,58c],
G. Brandt[177], O. Brandt[30], F. Braren[44], B. Brau[99], J.E. Brau[127], W.D. Breaden Madden[55],
K. Brendlinger[44], R. Brener[175], L. Brenner[34], R. Brenner[167], S. Bressler[175], B. Brickwedde[96],
D.L. Briglin[19], D. Britton[55], D. Britzger[111], I. Brock[22], R. Brock[103], G. Brooijmans[37],
W.K. Brooks[142e], E. Brost[27], P.A. Bruckman de Renstrom[82], B. Brüers[44], D. Bruncko[26b],
A. Bruni[21b], G. Bruni[21b], M. Bruschi[21b], N. Bruscino[70a,70b], L. Bryngemark[149], T. Buanes[15],
Q. Buat[151], P. Buchholz[147], A.G. Buckley[55], I.A. Budagov[77], M.K. Bugge[129], O. Bulekov[108],
B.A. Bullard[57], S. Burdin[88], C.D. Burgard[44], A.M. Burger[125], B. Burghgrave[7], J.T.P. Burr[44],
C.D. Burton[10], J.C. Burzynski[148], E.L. Busch[37], V. Büscher[96], P.J. Bussey[55], J.M. Butler[23],
C.M. Buttar[55], J.M. Butterworth[92], W. Buttinger[139], C.J. Buxo Vazquez[103],
A.R. Buzykaev[117b,117a], G. Cabras[21b], S. Cabrera Urbán[169], D. Caforio[54], H. Cai[134],
V.M.M. Cairo[149], O. Cakir[3a], N. Calace[34], P. Calafiura[16], G. Calderini[131], P. Calfayan[63],
G. Callea[55], L.P. Caloba[78b], D. Calvet[36], S. Calvet[36], T.P. Calvet[98], M. Calvetti[69a,69b],
R. Camacho Toro[131], S. Camarda[34], D. Camarero Munoz[95], P. Camarri[71a,71b],
M.T. Camerlingo[72a,72b], D. Cameron[129], C. Camincher[171], M. Campanelli[92], A. Camplani[38],
V. Canale[67a,67b], A. Canesse[100], M. Cano Bret[75], J. Cantero[125], Y. Cao[168], F. Capocasa[24],
M. Capua[39b,39a], A. Carbone[66a,66b], R. Cardarelli[71a], J.C.J. Cardenas[7], F. Cardillo[169],
G. Carducci[39b,39a], T. Carli[34], G. Carlino[67a], B.T. Carlson[134], E.M. Carlson[171,163a],
L. Carminati[66a,66b], M. Carnesale[70a,70b], R.M.D. Carney[149], S. Caron[114], E. Carquin[142e],
S. Carrá[44], G. Carratta[21b,21a], J.W.S. Carter[162], T.M. Carter[48], D. Casadei[31c], M.P. Casado[12,g],
A.F. Casha[162], E.G. Castiglia[178], F.L. Castillo[59a], L. Castillo Garcia[12], V. Castillo Gimenez[169],
N.F. Castro[135a,135e], A. Catinaccio[34], J.R. Catmore[129], A. Cattai[34], V. Cavaliere[27],
N. Cavalli[21b,21a], V. Cavasinni[69a,69b], E. Celebi[11b], F. Celli[130], M.S. Centonze[65a,65b],
K. Cerny[126], A.S. Cerqueira[78a], A. Cerri[152], L. Cerrito[71a,71b], F. Cerutti[16], A. Cervelli[21b],
S.A. Cetin[11b], Z. Chadi[33a], D. Chakraborty[116], M. Chala[135f], J. Chan[176], W.S. Chan[115],
W.Y. Chan[88], J.D. Chapman[30], B. Chargeishvili[155b], D.G. Charlton[19], T.P. Charman[90],
M. Chatterjee[18], S. Chekanov[5], S.V. Chekulaev[163a], G.A. Chelkov[77,ae], A. Chen[102], B. Chen[157],
B. Chen[171], C. Chen[58a], C.H. Chen[76], H. Chen[13c], H. Chen[27], J. Chen[58c], J. Chen[24], S. Chen[132],
S.J. Chen[13c], X. Chen[58c], X. Chen[13b], Y. Chen[58a], Y-H. Chen[44], C.L. Cheng[176], H.C. Cheng[60a],
A. Cheplakov[77], E. Cheremushkina[44], E. Cherepanova[77], R. Cherkaoui El Moursli[33e], E. Cheu[6],
K. Cheung[61], L. Chevalier[140], V. Chiarella[49], G. Chiarelli[69a], G. Chiodini[65a], A.S. Chisholm[19],
A. Chitan[25b], Y.H. Chiu[171], M.V. Chizhov[77,s], K. Choi[10], A.R. Chomont[70a,70b], Y. Chou[99],
E.Y.S. Chow[115], T. Chowdhury[31f], L.D. Christopher[31f], M.C. Chu[60a], X. Chu[13a,13d],
J. Chudoba[136], J.J. Chwastowski[82], D. Cieri[111], K.M. Ciesla[82], V. Cindro[89], I.A. Cioară[25b],
A. Ciocio[16], F. Cirotto[67a,67b], Z.H. Citron[175,k], M. Citterio[66a], D.A. Ciubotaru[25b],
B.M. Ciungu[162], A. Clark[52], P.J. Clark[48], J.M. Clavijo Columbie[44], S.E. Clawson[97],
C. Clement[43a,43b], L. Clissa[21b,21a], Y. Coadou[98], M. Cobal[64a,64c], A. Coccaro[53b], J. Cochran[76],
R.F. Coelho Barrue[135a], R. Coelho Lopes De Sa[99], S. Coelli[66a], H. Cohen[157], A.E.C. Coimbra[34],

B. Cole[37], J. Collot[56], P. Conde Muiño[135a,135g], S.H. Connell[31c], I.A. Connelly[55], E.I. Conroy[130], F. Conventi[67a,ak], H.G. Cooke[19], A.M. Cooper-Sarkar[130], F. Cormier[170], L.D. Corpe[34], M. Corradi[70a,70b], E.E. Corrigan[94], F. Corriveau[100,y], M.J. Costa[169], F. Costanza[4], D. Costanzo[145], B.M. Cote[123], G. Cowan[91], J.W. Cowley[30], K. Cranmer[121], S. Crépé-Renaudin[56], F. Crescioli[131], M. Cristinziani[147], M. Cristoforetti[73a,73b,b], V. Croft[165], G. Crosetti[39b,39a], A. Cueto[34], T. Cuhadar Donszelmann[166], H. Cui[13a,13d], A.R. Cukierman[149], W.R. Cunningham[55], F. Curcio[39b,39a], P. Czodrowski[34], M.M. Czurylo[59b], M.J. Da Cunha Sargedas De Sousa[58a], J.V. Da Fonseca Pinto[78b], C. Da Via[97], W. Dabrowski[81a], T. Dado[45], S. Dahbi[31f], T. Dai[102], C. Dallapiccola[99], M. Dam[38], G. D'amen[27], V. D'Amico[72a,72b], J. Damp[96], J.R. Dandoy[132], M.F. Daneri[28], M. Danninger[148], V. Dao[34], G. Darbo[53b], S. Darmora[5], A. Dattagupta[127], S. D'Auria[66a,66b], C. David[163b], T. Davidek[138], D.R. Davis[47], B. Davis-Purcell[32], I. Dawson[90], K. De[7], R. De Asmundis[67a], M. De Beurs[115], S. De Castro[21b,21a], N. De Groot[114], P. de Jong[115], H. De la Torre[103], A. De Maria[13c], D. De Pedis[70a], A. De Salvo[70a], U. De Sanctis[71a,71b], M. De Santis[71a,71b], A. De Santo[152], J.B. De Vivie De Regie[56], D.V. Dedovich[77], J. Degens[115], A.M. Deiana[40], J. Del Peso[95], Y. Delabat Diaz[44], F. Deliot[140], C.M. Delitzsch[6], M. Della Pietra[67a,67b], D. Della Volpe[52], A. Dell'Acqua[34], L. Dell'Asta[66a,66b], M. Delmastro[4], P.A. Delsart[56], S. Demers[178], M. Demichev[77], S.P. Denisov[118], L. D'Eramo[116], D. Derendarz[82], J.E. Derkaoui[33d], F. Derue[131], P. Dervan[88], K. Desch[22], K. Dette[162], C. Deutsch[22], P.O. Deviveiros[34], F.A. Di Bello[70a,70b], A. Di Ciaccio[71a,71b], L. Di Ciaccio[4], A. Di Domenico[70a,70b], C. Di Donato[67a,67b], A. Di Girolamo[34], G. Di Gregorio[69a,69b], A. Di Luca[73a,73b], B. Di Micco[72a,72b], R. Di Nardo[72a,72b], C. Diaconu[98], F.A. Dias[115], T. Dias Do Vale[135a], M.A. Diaz[142a], F.G. Diaz Capriles[22], J. Dickinson[16], M. Didenko[169], E.B. Diehl[102], J. Dietrich[17], S. Díez Cornell[44], C. Diez Pardos[147], A. Dimitrievska[16], W. Ding[13b], J. Dingfelder[22], I-M. Dinu[25b], S.J. Dittmeier[59b], F. Dittus[34], F. Djama[98], T. Djobava[155b], J.I. Djuvsland[15], M.A.B. Do Vale[143], D. Dodsworth[24], C. Doglioni[94], J. Dolejsi[138], Z. Dolezal[138], M. Donadelli[78c], B. Dong[58c], J. Donini[36], A. D'onofrio[13c], M. D'Onofrio[88], J. Dopke[139], A. Doria[67a], M.T. Dova[86], A.T. Doyle[55], E. Drechsler[148], E. Dreyer[148], T. Dreyer[51], A.S. Drobac[165], D. Du[58a], T.A. du Pree[115], F. Dubinin[107], M. Dubovsky[26a], A. Dubreuil[52], E. Duchovni[175], G. Duckeck[110], O.A. Ducu[34,25b], D. Duda[111], A. Dudarev[34], M. D'uffizi[97], L. Duflot[62], M. Dührssen[34], C. Dülsen[177], A.E. Dumitriu[25b], M. Dunford[59a], S. Dungs[45], K. Dunne[43a,43b], A. Duperrin[98], H. Duran Yildiz[3a], M. Düren[54], A. Durglishvili[155b], B. Dutta[44], B.L. Dwyer[116], G.I. Dyckes[16], M. Dyndal[81a], S. Dysch[97], B.S. Dziedzic[82], B. Eckerova[26a], M.G. Eggleston[47], E. Egidio Purcino De Souza[78b], L.F. Ehrke[52], T. Eifert[7], G. Eigen[15], K. Einsweiler[16], T. Ekelof[167], Y. El Ghazali[33b], H. El Jarrari[33e], A. El Moussaouy[33a], V. Ellajosyula[167], M. Ellert[167], F. Ellinghaus[177], A.A. Elliot[90], N. Ellis[34], J. Elmsheuser[27], M. Elsing[34], D. Emeliyanov[139], A. Emerman[37], Y. Enari[159], J. Erdmann[45], A. Ereditato[18], P.A. Erland[82], M. Errenst[177], M. Escalier[62], C. Escobar[169], O. Estrada Pastor[169], E. Etzion[157], G. Evans[135a], H. Evans[63], M.O. Evans[152], A. Ezhilov[133], F. Fabbri[55], L. Fabbri[21b,21a], G. Facini[173], V. Fadeyev[141], R.M. Fakhrutdinov[118], S. Falciano[70a], P.J. Falke[22], S. Falke[34], J. Faltova[138], Y. Fan[13a], Y. Fang[13a], G. Fanourakis[42], M. Fanti[66a,66b], M. Faraj[58c], A. Farbin[7], A. Farilla[72a], E.M. Farina[68a,68b], T. Farooque[103], S.M. Farrington[48], P. Farthouat[34], F. Fassi[33e], D. Fassouliotis[8], M. Faucci Giannelli[71a,71b], W.J. Fawcett[30], L. Fayard[62], O.L. Fedin[133,p], G. Fedotov[133], M. Feickert[168], L. Feligioni[98], A. Fell[145], C. Feng[58b], M. Feng[13b], M.J. Fenton[166], A.B. Fenyuk[118], S.W. Ferguson[41], J. Ferrando[44], A. Ferrari[167], P. Ferrari[115], R. Ferrari[68a], D. Ferrere[52], C. Ferretti[102], F. Fiedler[96], A. Filipčič[89], F. Filthaut[114], M.C.N. Fiolhais[135a,135c,a], L. Fiorini[169], F. Fischer[147], W.C. Fisher[103], T. Fitschen[19], I. Fleck[147], P. Fleischmann[102], T. Flick[177], B.M. Flierl[110], L. Flores[132], M. Flores[31d], L.R. Flores Castillo[60a], F.M. Follega[73a,73b], N. Fomin[15], J.H. Foo[162], B.C. Forland[63], A. Formica[140], F.A. Förster[12],

A.C. Forti[97], E. Fortin[98], M.G. Foti[130], L. Fountas[8], D. Fournier[62], H. Fox[87],
P. Francavilla[69a,69b], S. Francescato[57], M. Franchini[21b,21a], S. Franchino[59a], D. Francis[34],
L. Franco[4], L. Franconi[18], M. Franklin[57], G. Frattari[70a,70b], A.C. Freegard[90], P.M. Freeman[19],
W.S. Freund[78b], E.M. Freundlich[45], D. Froidevaux[34], J.A. Frost[130], Y. Fu[58a], M. Fujimoto[122],
E. Fullana Torregrosa[169], J. Fuster[169], A. Gabrielli[21b,21a], A. Gabrielli[34], P. Gadow[44],
G. Gagliardi[53b,53a], L.G. Gagnon[16], G.E. Gallardo[130], E.J. Gallas[130], B.J. Gallop[139],
R. Gamboa Goni[90], K.K. Gan[123], S. Ganguly[159], J. Gao[58a], Y. Gao[48], Y.S. Gao[29,m],
F.M. Garay Walls[142a], C. García[169], J.E. García Navarro[169], J.A. García Pascual[13a],
M. Garcia-Sciveres[16], R.W. Gardner[35], D. Garg[75], R.B. Garg[149], S. Gargiulo[50], C.A. Garner[162],
V. Garonne[129], S.J. Gasiorowski[144], P. Gaspar[78b], G. Gaudio[68a], P. Gauzzi[70a,70b],
I.L. Gavrilenko[107], A. Gavrilyuk[119], C. Gay[170], G. Gaycken[44], E.N. Gazis[9], A.A. Geanta[25b],
C.M. Gee[141], C.N.P. Gee[139], J. Geisen[94], M. Geisen[96], C. Gemme[53b], M.H. Genest[56],
S. Gentile[70a,70b], S. George[91], W.F. George[19], T. Geralis[42], L.O. Gerlach[51],
P. Gessinger-Befurt[34], M. Ghasemi Bostanabad[171], A. Ghosh[166], A. Ghosh[75], B. Giacobbe[21b],
S. Giagu[70a,70b], N. Giangiacomi[162], P. Giannetti[69a], A. Giannini[67a,67b], S.M. Gibson[91],
M. Gignac[141], D.T. Gil[81b], B.J. Gilbert[37], D. Gillberg[32], G. Gilles[115], N.E.K. Gillwald[44],
D.M. Gingrich[2,aj], M.P. Giordani[64a,64c], P.F. Giraud[140], G. Giugliarelli[64a,64c], D. Giugni[66a],
F. Giuli[71a,71b], I. Gkialas[8,h], P. Gkountoumis[9], L.K. Gladilin[109], C. Glasman[95], G.R. Gledhill[127],
M. Glisic[127], I. Gnesi[39b,d], M. Goblirsch-Kolb[24], D. Godin[106], S. Goldfarb[101], T. Golling[52],
D. Golubkov[118], J.P. Gombas[103], A. Gomes[135a,135b], R. Goncalves Gama[51], R. Gonçalo[135a,135c],
G. Gonella[127], L. Gonella[19], A. Gongadze[77], F. Gonnella[19], J.L. Gonski[37],
S. González de la Hoz[169], S. Gonzalez Fernandez[12], R. Gonzalez Lopez[88], C. Gonzalez Renteria[16],
R. Gonzalez Suarez[167], S. Gonzalez-Sevilla[52], G.R. Gonzalvo Rodriguez[169],
R.Y. González Andana[142a], L. Goossens[34], N.A. Gorasia[19], P.A. Gorbounov[119], H.A. Gordon[27],
B. Gorini[34], E. Gorini[65a,65b], A. Gorišek[89], A.T. Goshaw[47], M.I. Gostkin[77], C.A. Gottardo[114],
M. Gouighri[33b], V. Goumarre[44], A.G. Goussiou[144], N. Govender[31c], C. Goy[4],
I. Grabowska-Bold[81a], K. Graham[32], E. Gramstad[129], S. Grancagnolo[17], M. Grandi[152],
V. Gratchev[133], P.M. Gravila[25f], F.G. Gravili[65a,65b], H.M. Gray[16], C. Grefe[22], I.M. Gregor[44],
P. Grenier[149], K. Grevtsov[44], C. Grieco[12], N.A. Grieser[124], A.A. Grillo[141], K. Grimm[29,l],
S. Grinstein[12,v], J.-F. Grivaz[62], S. Groh[96], E. Gross[175], J. Grosse-Knetter[51], C. Grud[102],
A. Grummer[113], J.C. Grundy[130], L. Guan[102], W. Guan[176], C. Gubbels[170], J. Guenther[34],
J.G.R. Guerrero Rojas[169], F. Guescini[111], D. Guest[17], R. Gugel[96], A. Guida[44], T. Guillemin[4],
S. Guindon[34], J. Guo[58c], L. Guo[62], Y. Guo[102], R. Gupta[44], S. Gurbuz[22], G. Gustavino[124],
M. Guth[52], P. Gutierrez[124], L.F. Gutierrez Zagazeta[132], C. Gutschow[92], C. Guyot[140],
C. Gwenlan[130], C.B. Gwilliam[88], E.S. Haaland[129], A. Haas[121], M. Habedank[44], C. Haber[16],
H.K. Hadavand[7], A. Hadef[96], S. Hadzic[111], M. Haleem[172], J. Haley[125], J.J. Hall[145],
G. Halladjian[103], G.D. Hallewell[98], L. Halser[18], K. Hamano[171], H. Hamdaoui[33e], M. Hamer[22],
G.N. Hamity[48], K. Han[58a], L. Han[13c], L. Han[58a], S. Han[16], Y.F. Han[162], K. Hanagaki[79,t],
M. Hance[141], M.D. Hank[35], R. Hankache[97], E. Hansen[94], J.B. Hansen[38], J.D. Hansen[38],
M.C. Hansen[22], P.H. Hansen[38], K. Hara[164], T. Harenberg[177], S. Harkusha[104], Y.T. Harris[130],
P.F. Harrison[173], N.M. Hartman[149], N.M. Hartmann[110], Y. Hasegawa[146], A. Hasib[48],
S. Hassani[140], S. Haug[18], R. Hauser[103], M. Havranek[137], C.M. Hawkes[19], R.J. Hawkings[34],
S. Hayashida[112], D. Hayden[103], C. Hayes[102], R.L. Hayes[170], C.P. Hays[130], J.M. Hays[90],
H.S. Hayward[88], S.J. Haywood[139], F. He[58a], Y. He[160], Y. He[131], M.P. Heath[48], V. Hedberg[94],
A.L. Heggelund[129], N.D. Hehir[90], C. Heidegger[50], K.K. Heidegger[50], W.D. Heidorn[76],
J. Heilman[32], S. Heim[44], T. Heim[16], B. Heinemann[44,ah], J.G. Heinlein[132], J.J. Heinrich[127],
L. Heinrich[34], J. Hejbal[136], L. Helary[44], A. Held[121], C.M. Helling[141], S. Hellman[43a,43b],
C. Helsens[34], R.C.W. Henderson[87], L. Henkelmann[30], A.M. Henriques Correia[34], H. Herde[149],
Y. Hernández Jiménez[151], H. Herr[96], M.G. Herrmann[110], T. Herrmann[46], G. Herten[50],

R. Hertenberger[110], L. Hervas[34], N.P. Hessey[163a], H. Hibi[80], S. Higashino[79],
E. Higón-Rodriguez[169], K.H. Hiller[44], S.J. Hillier[19], M. Hils[46], I. Hinchliffe[16], F. Hinterkeuser[22],
M. Hirose[128], S. Hirose[164], D. Hirschbuehl[177], B. Hiti[89], O. Hladik[136], J. Hobbs[151],
R. Hobincu[25e], N. Hod[175], M.C. Hodgkinson[145], B.H. Hodkinson[30], A. Hoecker[34], J. Hofer[44],
D. Hohn[50], T. Holm[22], T.R. Holmes[35], M. Holzbock[111], L.B.A.H. Hommels[30], B.P. Honan[97],
J. Hong[58c], T.M. Hong[134], Y. Hong[51], J.C. Honig[50], A. Hönle[111], B.H. Hooberman[168],
W.H. Hopkins[5], Y. Horii[112], L.A. Horyn[35], S. Hou[154], J. Howarth[55], J. Hoya[86], M. Hrabovsky[126],
A. Hrynevich[105], T. Hryn'ova[4], P.J. Hsu[61], S.-C. Hsu[144], Q. Hu[37], S. Hu[58c], Y.F. Hu[13a,13d,al],
D.P. Huang[92], X. Huang[13c], Y. Huang[58a], Y. Huang[13a], Z. Hubacek[137], F. Hubaut[98],
M. Huebner[22], F. Huegging[22], T.B. Huffman[130], M. Huhtinen[34], S.K. Huiberts[15], R. Hulsken[56],
N. Huseynov[77,z], J. Huston[103], J. Huth[57], R. Hyneman[149], S. Hyrych[26a], G. Iacobucci[52],
G. Iakovidis[27], I. Ibragimov[147], L. Iconomidou-Fayard[62], P. Iengo[34], R. Iguchi[159], T. Iizawa[52],
Y. Ikegami[79], A. Ilg[18], N. Ilic[162], H. Imam[33a], T. Ingebretsen Carlson[43a,43b], G. Introzzi[68a,68b],
M. Iodice[72a], V. Ippolito[70a,70b], M. Ishino[159], W. Islam[176], C. Issever[17,44], S. Istin[11c,am],
J.M. Iturbe Ponce[60a], R. Iuppa[73a,73b], A. Ivina[175], J.M. Izen[41], V. Izzo[67a], P. Jacka[136],
P. Jackson[1], R.M. Jacobs[44], B.P. Jaeger[148], C.S. Jagfeld[110], G. Jäkel[177], K. Jakobs[50],
T. Jakoubek[175], J. Jamieson[55], K.W. Janas[81a], G. Jarlskog[94], A.E. Jaspan[88], N. Javadov[77,z],
T. Javůrek[34], M. Javurkova[99], F. Jeanneau[140], L. Jeanty[127], J. Jejelava[155a,aa], P. Jenni[50,e],
S. Jézéquel[4], J. Jia[151], Z. Jia[13c], Y. Jiang[58a], S. Jiggins[48], J. Jimenez Pena[111], S. Jin[13c],
A. Jinaru[25b], O. Jinnouchi[160], H. Jivan[31f], P. Johansson[145], K.A. Johns[6], C.A. Johnson[63],
D.M. Jones[30], E. Jones[173], R.W.L. Jones[87], T.J. Jones[88], J. Jovicevic[14], X. Ju[16],
J.J. Junggeburth[34], A. Juste Rozas[12,v], S. Kabana[142d], A. Kaczmarska[82], M. Kado[70a,70b],
H. Kagan[123], M. Kagan[149], A. Kahn[37], A. Kahn[132], C. Kahra[96], T. Kaji[174], E. Kajomovitz[156],
C.W. Kalderon[27], A. Kamenshchikov[118], M. Kaneda[159], N.J. Kang[141], S. Kang[76], Y. Kano[112],
D. Kar[31f], K. Karava[130], M.J. Kareem[163b], I. Karkanias[158], S.N. Karpov[77], Z.M. Karpova[77],
V. Kartvelishvili[87], A.N. Karyukhin[118], E. Kasimi[158], C. Kato[58d], J. Katzy[44], K. Kawade[146],
K. Kawagoe[85], T. Kawaguchi[112], T. Kawamoto[140], G. Kawamura[51], E.F. Kay[171], F.I. Kaya[165],
S. Kazakos[12], V.F. Kazanin[117b,117a], Y. Ke[151], J.M. Keaveney[31a], R. Keeler[171], J.S. Keller[32],
A.S. Kelly[92], D. Kelsey[152], J.J. Kempster[19], J. Kendrick[19], K.E. Kennedy[37], O. Kepka[136],
S. Kersten[177], B.P. Kerševan[89], S. Ketabchi Haghighat[162], M. Khandoga[131], A. Khanov[125],
A.G. Kharlamov[117b,117a], T. Kharlamova[117b,117a], E.E. Khoda[144], T.J. Khoo[17], G. Khoriauli[172],
E. Khramov[77], J. Khubua[155b], S. Kido[80], M. Kiehn[34], A. Kilgallon[127], E. Kim[160], Y.K. Kim[35],
N. Kimura[92], A. Kirchhoff[51], D. Kirchmeier[46], C. Kirfel[22], J. Kirk[139], A.E. Kiryunin[111],
T. Kishimoto[159], D.P. Kisliuk[162], C. Kitsaki[9], O. Kivernyk[22], T. Klapdor-Kleingrothaus[50],
M. Klassen[59a], C. Klein[32], L. Klein[172], M.H. Klein[102], M. Klein[88], U. Klein[88], P. Klimek[34],
A. Klimentov[27], F. Klimpel[111], T. Klingl[22], T. Klioutchnikova[34], F.F. Klitzner[110], P. Kluit[115],
S. Kluth[111], E. Kneringer[74], T.M. Knight[162], A. Knue[50], D. Kobayashi[85], R. Kobayashi[83],
M. Kobel[46], M. Kocian[149], T. Kodama[159], P. Kodys[138], D.M. Koeck[152], P.T. Koenig[22],
T. Koffas[32], N.M. Köhler[34], M. Kolb[140], I. Koletsou[4], T. Komarek[126], K. Köneke[50],
A.X.Y. Kong[1], T. Kono[122], V. Konstantinides[92], N. Konstantinidis[92], B. Konya[94],
R. Kopeliansky[63], S. Koperny[81a], K. Korcyl[82], K. Kordas[158], G. Koren[157], A. Korn[92], S. Korn[51],
I. Korolkov[12], E.V. Korolkova[145], N. Korotkova[109], B. Kortman[115], O. Kortner[111], S. Kortner[111],
W.H. Kostecka[116], V.V. Kostyukhin[147,161], A. Kotsokechagia[62], A. Kotwal[47], A. Koulouris[34],
A. Kourkoumeli-Charalampidi[68a,68b], C. Kourkoumelis[8], E. Kourlitis[5], O. Kovanda[152],
R. Kowalewski[171], W. Kozanecki[140], A.S. Kozhin[118], V.A. Kramarenko[109], G. Kramberger[89],
P. Kramer[96], D. Krasnopevtsev[58a], M.W. Krasny[131], A. Krasznahorkay[34], J.A. Kremer[96],
J. Kretzschmar[88], K. Kreul[17], P. Krieger[162], F. Krieter[110], S. Krishnamurthy[99], A. Krishnan[59b],
M. Krivos[138], K. Krizka[16], K. Kroeninger[45], H. Kroha[111], J. Kroll[136], J. Kroll[132],
K.S. Krowpman[103], U. Kruchonak[77], H. Krüger[22], N. Krumnack[76], M.C. Kruse[47],

J.A. Krzysiak[82], A. Kubota[160], O. Kuchinskaia[161], S. Kuday[3a], D. Kuechler[44], J.T. Kuechler[44], S. Kuehn[34], T. Kuhl[44], V. Kukhtin[77], Y. Kulchitsky[104,ad], S. Kuleshov[142c], M. Kumar[31f], N. Kumari[98], M. Kuna[56], A. Kupco[136], T. Kupfer[45], O. Kuprash[50], H. Kurashige[80], L.L. Kurchaninov[163a], Y.A. Kurochkin[104], A. Kurova[108], M.G. Kurth[13a,13d], E.S. Kuwertz[34], M. Kuze[160], A.K. Kvam[144], J. Kvita[126], T. Kwan[100], K.W. Kwok[60a], C. Lacasta[169], F. Lacava[70a,70b], H. Lacker[17], D. Lacour[131], N.N. Lad[92], E. Ladygin[77], R. Lafaye[4], B. Laforge[131], T. Lagouri[142d], S. Lai[51], I.K. Lakomiec[81a], N. Lalloue[56], J.E. Lambert[124], S. Lammers[63], W. Lampl[6], C. Lampoudis[158], E. Lançon[27], U. Landgraf[50], M.P.J. Landon[90], V.S. Lang[50], J.C. Lange[51], R.J. Langenberg[99], A.J. Lankford[166], F. Lanni[27], K. Lantzsch[22], A. Lanza[68a], A. Lapertosa[53b,53a], J.F. Laporte[140], T. Lari[66a], F. Lasagni Manghi[21b], M. Lassnig[34], V. Latonova[136], T.S. Lau[60a], A. Laudrain[96], A. Laurier[32], M. Lavorgna[67a,67b], S.D. Lawlor[91], Z. Lawrence[97], M. Lazzaroni[66a,66b], B. Le[97], B. Leban[89], A. Lebedev[76], M. LeBlanc[34], T. LeCompte[5], F. Ledroit-Guillon[56], A.C.A. Lee[92], G.R. Lee[15], L. Lee[57], S.C. Lee[154], S. Lee[76], L.L. Leeuw[31c], B. Lefebvre[163a], H.P. Lefebvre[91], M. Lefebvre[171], C. Leggett[16], K. Lehmann[148], N. Lehmann[18], G. Lehmann Miotto[34], W.A. Leight[44], A. Leisos[158,u], M.A.L. Leite[78c], C.E. Leitgeb[44], R. Leitner[138], K.J.C. Leney[40], T. Lenz[22], S. Leone[69a], C. Leonidopoulos[48], A. Leopold[150], C. Leroy[106], R. Les[103], C.G. Lester[30], M. Levchenko[133], J. Levêque[4], D. Levin[102], L.J. Levinson[175], D.J. Lewis[19], B. Li[13b], B. Li[58b], C. Li[58a], C-Q. Li[58c,58d], H. Li[58a], H. Li[58b], H. Li[58b], J. Li[58c], K. Li[144], L. Li[58c], M. Li[13a,13d], Q.Y. Li[58a], S. Li[58d,58c,c], T. Li[58b], X. Li[44], Y. Li[44], Z. Li[58b], Z. Li[130], Z. Li[100], Z. Li[88], Z. Liang[13a], M. Liberatore[44], B. Liberti[71a], K. Lie[60c], J. Lieber Marin[78b], K. Lin[103], R.A. Linck[63], R.E. Lindley[6], J.H. Lindon[2], A. Linss[44], E. Lipeles[132], A. Lipniacka[15], T.M. Liss[168,ai], A. Lister[170], J.D. Little[7], B. Liu[13a], B.X. Liu[148], J.B. Liu[58a], J.K.K. Liu[35], K. Liu[58d,58c], M. Liu[58a], M.Y. Liu[58a], P. Liu[13a], X. Liu[58a], Y. Liu[44], Y. Liu[13c,13d], Y.L. Liu[102], Y.W. Liu[58a], M. Livan[68a,68b], J. Llorente Merino[148], S.L. Lloyd[90], E.M. Lobodzinska[44], P. Loch[6], S. Loffredo[71a,71b], T. Lohse[17], K. Lohwasser[145], M. Lokajicek[136], J.D. Long[168], I. Longarini[70a,70b], L. Longo[34], R. Longo[168], I. Lopez Paz[12], A. Lopez Solis[44], J. Lorenz[110], N. Lorenzo Martinez[4], A.M. Lory[110], A. Lösle[50], X. Lou[43a,43b], X. Lou[13a], A. Lounis[62], J. Love[5], P.A. Love[87], J.J. Lozano Bahilo[169], G. Lu[13a], M. Lu[58a], S. Lu[132], Y.J. Lu[61], H.J. Lubatti[144], C. Luci[70a,70b], F.L. Lucio Alves[13c], A. Lucotte[56], F. Luehring[63], I. Luise[151], L. Luminari[70a], O. Lundberg[150], B. Lund-Jensen[150], N.A. Luongo[127], M.S. Lutz[157], D. Lynn[27], H. Lyons[88], R. Lysak[136], E. Lytken[94], F. Lyu[13a], V. Lyubushkin[77], T. Lyubushkina[77], H. Ma[27], L.L. Ma[58b], Y. Ma[92], D.M. Mac Donell[171], G. Maccarrone[49], C.M. Macdonald[145], J.C. MacDonald[145], R. Madar[36], W.F. Mader[46], M. Madugoda Ralalage Don[125], N. Madysa[46], J. Maeda[80], T. Maeno[27], M. Maerker[46], V. Magerl[50], J. Magro[64a,64c], D.J. Mahon[37], C. Maidantchik[78b], A. Maio[135a,135b,135d], K. Maj[81a], O. Majersky[26a], S. Majewski[127], N. Makovec[62], V. Maksimovic[14], B. Malaescu[131], Pa. Malecki[82], V.P. Maleev[133], F. Malek[56], D. Malito[39b,39a], U. Mallik[75], C. Malone[30], S. Maltezos[9], S. Malyukov[77], J. Mamuzic[169], G. Mancini[49], J.P. Mandalia[90], I. Mandić[89], L. Manhaes de Andrade Filho[78a], I.M. Maniatis[158], M. Manisha[140], J. Manjarres Ramos[46], K.H. Mankinen[94], A. Mann[110], A. Manousos[74], B. Mansoulie[140], I. Manthos[158], S. Manzoni[115], A. Marantis[158,u], G. Marchiori[131], M. Marcisovsky[136], L. Marcoccia[71a,71b], C. Marcon[94], M. Marjanovic[124], Z. Marshall[16], S. Marti-Garcia[169], T.A. Martin[173], V.J. Martin[48], B. Martin dit Latour[15], L. Martinelli[70a,70b], M. Martinez[12,v], P. Martinez Agullo[169], V.I. Martinez Outschoorn[99], S. Martin-Haugh[139], V.S. Martoiu[25b], A.C. Martyniuk[92], A. Marzin[34], S.R. Maschek[111], L. Masetti[96], T. Mashimo[159], J. Masik[97], A.L. Maslennikov[117b,117a], L. Massa[21b], P. Massarotti[67a,67b], P. Mastrandrea[69a,69b], A. Mastroberardino[39b,39a], T. Masubuchi[159], D. Matakias[27], T. Mathisen[167], A. Matic[110], N. Matsuzawa[159], J. Maurer[25b], B. Maček[89], D.A. Maximov[117b,117a], R. Mazini[154], I. Maznas[158], S.M. Mazza[141], C. Mc Ginn[27], J.P. Mc Gowan[100], S.P. Mc Kee[102], T.G. McCarthy[111], W.P. McCormack[16], E.F. McDonald[101], A.E. McDougall[115], J.A. Mcfayden[152],

G. Mchedlidze[155b], M.A. McKay[40], K.D. McLean[171], S.J. McMahon[139], P.C. McNamara[101],
R.A. McPherson[171,y], J.E. Mdhluli[31f], Z.A. Meadows[99], S. Meehan[34], T. Megy[36], S. Mehlhase[110],
A. Mehta[88], B. Meirose[41], D. Melini[156], B.R. Mellado Garcia[31f], A.H. Melo[51], F. Meloni[44],
A. Melzer[22], E.D. Mendes Gouveia[135a], A.M. Mendes Jacques Da Costa[19], H.Y. Meng[162],
L. Meng[34], S. Menke[111], M. Mentink[34], E. Meoni[39b,39a], C. Merlassino[130], P. Mermod[52,*],
L. Merola[67a,67b], C. Meroni[66a], G. Merz[102], O. Meshkov[107,109], J.K.R. Meshreki[147], J. Metcalfe[5],
A.S. Mete[5], C. Meyer[63], J-P. Meyer[140], M. Michetti[17], R.P. Middleton[139], L. Mijović[48],
G. Mikenberg[175], M. Mikestikova[136], M. Mikuž[89], H. Mildner[145], A. Milic[162], C.D. Milke[40],
D.W. Miller[35], L.S. Miller[32], A. Milov[175], D.A. Milstead[43a,43b], T. Min[13c], A.A. Minaenko[118],
I.A. Minashvili[155b], L. Mince[55], A.I. Mincer[121], B. Mindur[81a], M. Mineev[77], Y. Minegishi[159],
Y. Mino[83], L.M. Mir[12], M. Miralles Lopez[169], M. Mironova[130], T. Mitani[174], V.A. Mitsou[169],
M. Mittal[58c], O. Miu[162], P.S. Miyagawa[90], Y. Miyazaki[85], A. Mizukami[79], J.U. Mjörnmark[94],
T. Mkrtchyan[59a], M. Mlynarikova[116], T. Moa[43a,43b], S. Mobius[51], K. Mochizuki[106], P. Moder[44],
P. Mogg[110], A.F. Mohammed[13a], S. Mohapatra[37], G. Mokgatitswane[31f], B. Mondal[147],
S. Mondal[137], K. Mönig[44], E. Monnier[98], L. Monsonis Romero[169], A. Montalbano[148],
J. Montejo Berlingen[34], M. Montella[123], F. Monticelli[86], N. Morange[62],
A.L. Moreira De Carvalho[135a], M. Moreno Llácer[169], C. Moreno Martinez[12], P. Morettini[53b],
S. Morgenstern[173], D. Mori[148], M. Morii[57], M. Morinaga[159], V. Morisbak[129], A.K. Morley[34],
A.P. Morris[92], L. Morvaj[34], P. Moschovakos[34], B. Moser[115], M. Mosidze[155b], T. Moskalets[50],
P. Moskvitina[114], J. Moss[29,n], E.J.W. Moyse[99], S. Muanza[98], J. Mueller[134], R. Mueller[18],
D. Muenstermann[87], G.A. Mullier[94], J.J. Mullin[132], D.P. Mungo[66a,66b], J.L. Munoz Martinez[12],
F.J. Munoz Sanchez[97], M. Murin[97], P. Murin[26b], W.J. Murray[173,139], A. Murrone[66a,66b],
J.M. Muse[124], M. Muškinja[16], C. Mwewa[27], A.G. Myagkov[118,ae], A.J. Myers[7], A.A. Myers[134],
G. Myers[63], M. Myska[137], B.P. Nachman[16], O. Nackenhorst[45], A.Nag Nag[46], K. Nagai[130],
K. Nagano[79], J.L. Nagle[27], E. Nagy[98], A.M. Nairz[34], Y. Nakahama[112], K. Nakamura[79],
H. Nanjo[128], F. Napolitano[59a], R. Narayan[40], E.A. Narayanan[113], I. Naryshkin[133], M. Naseri[32],
C. Nass[22], T. Naumann[44], G. Navarro[20a], J. Navarro-Gonzalez[169], R. Nayak[157],
P.Y. Nechaeva[107], F. Nechansky[44], T.J. Neep[19], A. Negri[68a,68b], M. Negrini[21b], C. Nellist[114],
C. Nelson[100], K. Nelson[102], S. Nemecek[136], M. Nessi[34,f], M.S. Neubauer[168], F. Neuhaus[96],
J. Neundorf[44], R. Newhouse[170], P.R. Newman[19], C.W. Ng[134], Y.S. Ng[17], Y.W.Y. Ng[166],
B. Ngair[33e], H.D.N. Nguyen[106], R.B. Nickerson[130], R. Nicolaidou[140], D.S. Nielsen[38],
J. Nielsen[141], M. Niemeyer[51], N. Nikiforou[10], V. Nikolaenko[118,ae], I. Nikolic-Audit[131],
K. Nikolopoulos[19], P. Nilsson[27], H.R. Nindhito[52], A. Nisati[70a], N. Nishu[2], R. Nisius[111],
T. Nitta[174], T. Nobe[159], D.L. Noel[30], Y. Noguchi[83], I. Nomidis[131], M.A. Nomura[27],
M.B. Norfolk[145], R.R.B. Norisam[92], J. Novak[89], T. Novak[44], O. Novgorodova[46], L. Novotny[137],
R. Novotny[113], L. Nozka[126], K. Ntekas[166], E. Nurse[92], F.G. Oakham[32,aj], J. Ocariz[131],
A. Ochi[80], I. Ochoa[135a], J.P. Ochoa-Ricoux[142a], S. Oda[85], S. Odaka[79], S. Oerdek[167],
A. Ogrodnik[81a], A. Oh[97], C.C. Ohm[150], H. Oide[160], R. Oishi[159], M.L. Ojeda[44], Y. Okazaki[83],
M.W. O'Keefe[88], Y. Okumura[159], A. Olariu[25b], L.F. Oleiro Seabra[135a], S.A. Olivares Pino[142d],
D. Oliveira Damazio[27], D. Oliveira Goncalves[78a], J.L. Oliver[166], M.J.R. Olsson[166],
A. Olszewski[82], J. Olszowska[82], Ö.O. Öncel[22], D.C. O'Neil[148], A.P. O'neill[130], A. Onofre[135a,135e],
P.U.E. Onyisi[10], R.G. Oreamuno Madriz[116], M.J. Oreglia[35], G.E. Orellana[86], D. Orestano[72a,72b],
N. Orlando[12], R.S. Orr[162], V. O'Shea[55], R. Ospanov[58a], G. Otero y Garzon[28], H. Otono[85],
P.S. Ott[59a], G.J. Ottino[16], M. Ouchrif[33d], J. Ouellette[27], F. Ould-Saada[129], A. Ouraou[140,*],
Q. Ouyang[13a], M. Owen[55], R.E. Owen[139], K.Y. Oyulmaz[11c], V.E. Ozcan[11c], N. Ozturk[7],
S. Ozturk[11c], J. Pacalt[126], H.A. Pacey[30], K. Pachal[47], A. Pacheco Pages[12], C. Padilla Aranda[12],
S. Pagan Griso[16], G. Palacino[63], S. Palazzo[48], S. Palestini[34], M. Palka[81b], P. Palni[81a],
D.K. Panchal[10], C.E. Pandini[52], J.G. Panduro Vazquez[91], P. Pani[44], G. Panizzo[64a,64c],
L. Paolozzi[52], C. Papadatos[106], S. Parajuli[40], A. Paramonov[5], C. Paraskevopoulos[9],

D. Paredes Hernandez[60b], S.R. Paredes Saenz[130], B. Parida[175], T.H. Park[162], A.J. Parker[29],
M.A. Parker[30], F. Parodi[53b,53a], E.W. Parrish[116], J.A. Parsons[37], U. Parzefall[50],
L. Pascual Dominguez[157], V.R. Pascuzzi[16], F. Pasquali[115], E. Pasqualucci[70a], S. Passaggio[53b],
F. Pastore[91], P. Pasuwan[43a,43b], J.R. Pater[97], A. Pathak[176], J. Patton[88], T. Pauly[34],
J. Pearkes[149], M. Pedersen[129], L. Pedraza Diaz[114], R. Pedro[135a], T. Peiffer[51],
S.V. Peleganchuk[117b,117a], O. Penc[136], C. Peng[60b], H. Peng[58a], M. Penzin[161], B.S. Peralva[78a],
A.P. Pereira Peixoto[135a], L. Pereira Sanchez[43a,43b], D.V. Perepelitsa[27], E. Perez Codina[163a],
M. Perganti[9], L. Perini[66a,66b], H. Pernegger[34], S. Perrella[34], A. Perrevoort[115], K. Peters[44],
R.F.Y. Peters[97], B.A. Petersen[34], T.C. Petersen[38], E. Petit[98], V. Petousis[137], C. Petridou[158],
P. Petroff[62], F. Petrucci[72a,72b], A. Petrukhin[147], M. Pettee[178], N.E. Pettersson[34],
K. Petukhova[138], A. Peyaud[140], R. Pezoa[142e], L. Pezzotti[34], G. Pezzullo[178], T. Pham[101],
P.W. Phillips[139], M.W. Phipps[168], G. Piacquadio[151], E. Pianori[16], F. Piazza[66a,66b], A. Picazio[99],
R. Piegaia[28], D. Pietreanu[25b], J.E. Pilcher[35], A.D. Pilkington[97], M. Pinamonti[64a,64c],
J.L. Pinfold[2], C. Pitman Donaldson[92], D.A. Pizzi[32], L. Pizzimento[71a,71b], A. Pizzini[115],
M.-A. Pleier[27], V. Plesanovs[50], V. Pleskot[138], E. Plotnikova[77], P. Podberezko[117b,117a],
R. Poettgen[94], R. Poggi[52], L. Poggioli[131], I. Pogrebnyak[103], D. Pohl[22], I. Pokharel[51],
G. Polesello[68a], A. Poley[148,163a], A. Policicchio[70a,70b], R. Polifka[138], A. Polini[21b],
C.S. Pollard[130], Z.B. Pollock[123], V. Polychronakos[27], D. Ponomarenko[108], L. Pontecorvo[34],
S. Popa[25a], G.A. Popeneciu[25d], L. Portales[4], D.M. Portillo Quintero[163a], S. Pospisil[137],
P. Postolache[25c], K. Potamianos[130], I.N. Potrap[77], C.J. Potter[30], H. Potti[1], T. Poulsen[44],
J. Poveda[169], T.D. Powell[145], G. Pownall[44], M.E. Pozo Astigarraga[34], A. Prades Ibanez[169],
P. Pralavorio[98], M.M. Prapa[42], S. Prell[76], D. Price[97], M. Primavera[65a], M.A. Principe Martin[95],
M.L. Proffitt[144], N. Proklova[108], K. Prokofiev[60c], F. Prokoshin[77], S. Protopopescu[27],
J. Proudfoot[5], M. Przybycien[81a], D. Pudzha[133], P. Puzo[62], D. Pyatiizbyantseva[108], J. Qian[102],
Y. Qin[97], T. Qiu[90], A. Quadt[51], M. Queitsch-Maitland[34], G. Rabanal Bolanos[57],
F. Ragusa[66a,66b], J.A. Raine[52], S. Rajagopalan[27], K. Ran[13a,13d], D.F. Rassloff[59a], D.M. Rauch[44],
S. Rave[96], B. Ravina[55], I. Ravinovich[175], M. Raymond[34], A.L. Read[129], N.P. Readioff[145],
D.M. Rebuzzi[68a,68b], G. Redlinger[27], K. Reeves[41], D. Reikher[157], A. Reiss[96], A. Rej[147],
C. Rembser[34], A. Renardi[44], M. Renda[25b], M.B. Rendel[111], A.G. Rennie[55], S. Resconi[66a],
M. Ressegotti[53b,53a], E.D. Resseguie[16], S. Rettie[92], B. Reynolds[123], E. Reynolds[19],
M. Rezaei Estabragh[177], O.L. Rezanova[117b,117a], P. Reznicek[138], E. Ricci[73a,73b], R. Richter[111],
S. Richter[44], E. Richter-Was[81b], M. Ridel[131], P. Rieck[111], P. Riedler[34], O. Rifki[44],
M. Rijssenbeek[151], A. Rimoldi[68a,68b], M. Rimoldi[44], L. Rinaldi[21b,21a], T.T. Rinn[168],
M.P. Rinnagel[110], G. Ripellino[150], I. Riu[12], P. Rivadeneira[44], J.C. Rivera Vergara[171],
F. Rizatdinova[125], E. Rizvi[90], C. Rizzi[52], B.A. Roberts[173], B.R. Roberts[16], S.H. Robertson[100,y],
M. Robin[44], D. Robinson[30], C.M. Robles Gajardo[142e], M. Robles Manzano[96], A. Robson[55],
A. Rocchi[71a,71b], C. Roda[69a,69b], S. Rodriguez Bosca[59a], A. Rodriguez Rodriguez[50],
A.M. Rodríguez Vera[163b], S. Roe[34], A.R. Roepe[124], J. Roggel[177], O. Røhne[129], R.A. Rojas[171],
B. Roland[50], C.P.A. Roland[63], J. Roloff[27], A. Romaniouk[108], M. Romano[21b],
A.C. Romero Hernandez[168], N. Rompotis[88], M. Ronzani[121], L. Roos[131], S. Rosati[70a],
B.J. Rosser[132], E. Rossi[162], E. Rossi[4], E. Rossi[67a,67b], L.P. Rossi[53b], L. Rossini[44], R. Rosten[123],
M. Rotaru[25b], B. Rottler[50], D. Rousseau[62], D. Rousso[30], G. Rovelli[68a,68b], A. Roy[10],
A. Rozanov[98], Y. Rozen[156], X. Ruan[31f], A.J. Ruby[88], T.A. Ruggeri[1], F. Rühr[50],
A. Ruiz-Martinez[169], A. Rummler[34], Z. Rurikova[50], N.A. Rusakovich[77], H.L. Russell[34],
L. Rustige[36], J.P. Rutherfoord[6], E.M. Rüttinger[145], M. Rybar[138], E.B. Rye[129], A. Ryzhov[118],
J.A. Sabater Iglesias[44], P. Sabatini[169], L. Sabetta[70a,70b], H.F-W. Sadrozinski[141], R. Sadykov[77],
F. Safai Tehrani[70a], B. Safarzadeh Samani[152], M. Safdari[149], S. Saha[100], M. Sahinsoy[111],
A. Sahu[177], M. Saimpert[140], M. Saito[159], T. Saito[159], D. Salamani[34], G. Salamanna[72a,72b],
A. Salnikov[149], J. Salt[169], A. Salvador Salas[12], D. Salvatore[39b,39a], F. Salvatore[152],

A. Salzburger[34], D. Sammel[50], D. Sampsonidis[158], D. Sampsonidou[58d,58c], J. Sánchez[169],
A. Sanchez Pineda[4], V. Sanchez Sebastian[169], H. Sandaker[129], C.O. Sander[44],
I.G. Sanderswood[87], J.A. Sandesara[99], M. Sandhoff[177], C. Sandoval[20b], D.P.C. Sankey[139],
M. Sannino[53b,53a], A. Sansoni[49], C. Santoni[36], H. Santos[135a,135b], S.N. Santpur[16], A. Santra[175],
K.A. Saoucha[145], A. Sapronov[77], J.G. Saraiva[135a,135d], J. Sardain[98], O. Sasaki[79], K. Sato[164],
C. Sauer[59b], F. Sauerburger[50], E. Sauvan[4], P. Savard[162,aj], R. Sawada[159], C. Sawyer[139],
L. Sawyer[93], I. Sayago Galvan[169], C. Sbarra[21b], A. Sbrizzi[21b,21a], T. Scanlon[92],
J. Schaarschmidt[144], P. Schacht[111], D. Schaefer[35], U. Schäfer[96], A.C. Schaffer[62], D. Schaile[110],
R.D. Schamberger[151], E. Schanet[110], C. Scharf[17], N. Scharmberg[97], V.A. Schegelsky[133],
D. Scheirich[138], F. Schenck[17], M. Schernau[166], C. Schiavi[53b,53a], L.K. Schildgen[22],
Z.M. Schillaci[24], E.J. Schioppa[65a,65b], M. Schioppa[39b,39a], B. Schlag[96], K.E. Schleicher[50],
S. Schlenker[34], K. Schmieden[96], C. Schmitt[96], S. Schmitt[44], L. Schoeffel[140], A. Schoening[59b],
P.G. Scholer[50], E. Schopf[130], M. Schott[96], J. Schovancova[34], S. Schramm[52], F. Schroeder[177],
H-C. Schultz-Coulon[59a], M. Schumacher[50], B.A. Schumm[141], Ph. Schune[140], A. Schwartzman[149],
T.A. Schwarz[102], Ph. Schwemling[140], R. Schwienhorst[103], A. Sciandra[141], G. Sciolla[24],
F. Scuri[69a], F. Scutti[101], C.D. Sebastiani[88], K. Sedlaczek[45], P. Seema[17], S.C. Seidel[113],
A. Seiden[141], B.D. Seidlitz[27], T. Seiss[35], C. Seitz[44], J.M. Seixas[78b], G. Sekhniaidze[67a],
S.J. Sekula[40], L. Selem[4], N. Semprini-Cesari[21b,21a], S. Sen[47], C. Serfon[27], L. Serin[62],
L. Serkin[64a,64b], M. Sessa[72a,72b], H. Severini[124], S. Sevova[149], F. Sforza[53b,53a], A. Sfyrla[52],
E. Shabalina[51], R. Shaheen[150], J.D. Shahinian[132], N.W. Shaikh[43a,43b], D. Shaked Renous[175],
L.Y. Shan[13a], M. Shapiro[16], A. Sharma[34], A.S. Sharma[1], S. Sharma[44], P.B. Shatalov[119],
K. Shaw[152], S.M. Shaw[97], P. Sherwood[92], L. Shi[92], C.O. Shimmin[178], Y. Shimogama[174],
J.D. Shinner[91], I.P.J. Shipsey[130], S. Shirabe[52], M. Shiyakova[77], J. Shlomi[175], M.J. Shochet[35],
J. Shojaii[101], D.R. Shope[150], S. Shrestha[123], E.M. Shrif[31f], M.J. Shroff[171], E. Shulga[175],
P. Sicho[136], A.M. Sickles[168], E. Sideras Haddad[31f], O. Sidiropoulou[34], A. Sidoti[21b], F. Siegert[46],
Dj. Sijacki[14], J.M. Silva[19], M.V. Silva Oliveira[34], S.B. Silverstein[43a], S. Simion[62], R. Simoniello[34],
N.D. Simpson[94], S. Simsek[11b], P. Sinervo[162], V. Sinetckii[109], S. Singh[148], S. Singh[162], S. Sinha[44],
S. Sinha[31f], M. Sioli[21b,21a], I. Siral[127], S.Yu. Sivoklokov[109], J. Sjölin[43a,43b], A. Skaf[51],
E. Skorda[94], P. Skubic[124], M. Slawinska[82], K. Sliwa[165], V. Smakhtin[175], B.H. Smart[139],
J. Smiesko[138], S.Yu. Smirnov[108], Y. Smirnov[108], L.N. Smirnova[109,r], O. Smirnova[94],
E.A. Smith[35], H.A. Smith[130], M. Smizanska[87], K. Smolek[137], A. Smykiewicz[82], A.A. Snesarev[107],
H.L. Snoek[115], S. Snyder[27], R. Sobie[171,y], A. Soffer[157], F. Sohns[51], C.A. Solans Sanchez[34],
E.Yu. Soldatov[108], U. Soldevila[169], A.A. Solodkov[118], S. Solomon[50], A. Soloshenko[77],
O.V. Solovyanov[118], V. Solovyev[133], P. Sommer[145], H. Son[165], A. Sonay[12], W.Y. Song[163b],
A. Sopczak[137], A.L. Sopio[92], F. Sopkova[26b], S. Sottocornola[68a,68b], R. Soualah[64a,64c],
A.M. Soukharev[117b,117a], Z. Soumaimi[33e], D. South[44], S. Spagnolo[65a,65b], M. Spalla[111],
M. Spangenberg[173], F. Spanò[91], D. Sperlich[50], T.M. Spieker[59a], G. Spigo[34], M. Spina[152],
D.P. Spiteri[55], M. Spousta[138], A. Stabile[66a,66b], R. Stamen[59a], M. Stamenkovic[115],
A. Stampekis[19], M. Standke[22], E. Stanecka[82], B. Stanislaus[34], M.M. Stanitzki[44],
M. Stankaityte[130], B. Stapf[44], E.A. Starchenko[118], G.H. Stark[141], J. Stark[98], D.M. Starko[163b],
P. Staroba[136], P. Starovoitov[59a], S. Stärz[100], R. Staszewski[82], G. Stavropoulos[42], P. Steinberg[27],
A.L. Steinhebel[127], B. Stelzer[148,163a], H.J. Stelzer[134], O. Stelzer-Chilton[163a], H. Stenzel[54],
T.J. Stevenson[152], G.A. Stewart[34], M.C. Stockton[34], G. Stoicea[25b], M. Stolarski[135a],
S. Stonjek[111], A. Straessner[46], J. Strandberg[150], S. Strandberg[43a,43b], M. Strauss[124],
T. Strebler[98], P. Strizenec[26b], R. Ströhmer[172], D.M. Strom[127], L.R. Strom[44], R. Stroynowski[40],
A. Strubig[43a,43b], S.A. Stucci[27], B. Stugu[15], J. Stupak[124], N.A. Styles[44], D. Su[149], S. Su[58a],
W. Su[58d,144,58c], X. Su[58a], K. Sugizaki[159], V.V. Sulin[107], M.J. Sullivan[88], D.M.S. Sultan[52],
L. Sultanaliyeva[107], S. Sultansoy[3c], T. Sumida[83], S. Sun[102], S. Sun[176], X. Sun[97],
O. Sunneborn Gudnadottir[167], C.J.E. Suster[153], M.R. Sutton[152], M. Svatos[136],

M. Swiatlowski[163a], T. Swirski[172], I. Sykora[26a], M. Sykora[138], T. Sykora[138], D. Ta[96],
K. Tackmann[44,w], A. Taffard[166], R. Tafirout[163a], R.H.M. Taibah[131], R. Takashima[84],
K. Takeda[80], T. Takeshita[146], E.P. Takeva[48], Y. Takubo[79], M. Talby[98], A.A. Talyshev[117b,117a],
K.C. Tam[60b], N.M. Tamir[157], A. Tanaka[159], J. Tanaka[159], R. Tanaka[62], J. Tang[58c], Z. Tao[170],
S. Tapia Araya[76], S. Tapprogge[96], A. Tarek Abouelfadl Mohamed[103], S. Tarem[156], K. Tariq[58b],
G. Tarna[25b], G.F. Tartarelli[66a], P. Tas[138], M. Tasevsky[136], E. Tassi[39b,39a], G. Tateno[159],
Y. Tayalati[33e], G.N. Taylor[101], W. Taylor[163b], H. Teagle[88], A.S. Tee[176], R. Teixeira De Lima[149],
P. Teixeira-Dias[91], H. Ten Kate[34], J.J. Teoh[115], K. Terashi[159], J. Terron[95], S. Terzo[12],
M. Testa[49], R.J. Teuscher[162,y], N. Themistokleous[48], T. Theveneaux-Pelzer[17], O. Thielmann[177],
D.W. Thomas[91], J.P. Thomas[19], E.A. Thompson[44], P.D. Thompson[19], E. Thomson[132],
E.J. Thorpe[90], Y. Tian[51], V. Tikhomirov[107,af], Yu.A. Tikhonov[117b,117a], S. Timoshenko[108],
P. Tipton[178], S. Tisserant[98], S.H. Tlou[31f], A. Tnourji[36], K. Todome[21b,21a], S. Todorova-Nova[138],
S. Todt[46], M. Togawa[79], J. Tojo[85], S. Tokár[26a], K. Tokushuku[79], E. Tolley[123], R. Tombs[30],
M. Tomoto[79,112], L. Tompkins[149], P. Tornambe[99], E. Torrence[127], H. Torres[46],
E. Torró Pastor[169], M. Toscani[28], C. Tosciri[35], J. Toth[98,x], D.R. Tovey[145], A. Traeet[15],
C.J. Treado[121], T. Trefzger[172], A. Tricoli[27], I.M. Trigger[163a], S. Trincaz-Duvoid[131],
D.A. Trischuk[170], W. Trischuk[162], B. Trocmé[56], A. Trofymov[62], C. Troncon[66a], F. Trovato[152],
L. Truong[31c], M. Trzebinski[82], A. Trzupek[82], F. Tsai[151], A. Tsiamis[158], P.V. Tsiareshka[104,ad],
A. Tsirigotis[158,u], V. Tsiskaridze[151], E.G. Tskhadadze[155a], M. Tsopoulou[158], Y. Tsujikawa[83],
I.I. Tsukerman[119], V. Tsulaia[16], S. Tsuno[79], O. Tsur[156], D. Tsybychev[151], Y. Tu[60b],
A. Tudorache[25b], V. Tudorache[25b], A.N. Tuna[34], S. Turchikhin[77], I. Turk Cakir[3a], R.J. Turner[19],
R. Turra[66a], P.M. Tuts[37], S. Tzamarias[158], P. Tzanis[9], E. Tzovara[96], K. Uchida[159],
F. Ukegawa[164], P.A. Ulloa Poblete[142b], G. Unal[34], M. Unal[10], A. Undrus[27], G. Unel[166],
F.C. Ungaro[101], K. Uno[159], J. Urban[26b], P. Urquijo[101], G. Usai[7], R. Ushioda[160], M. Usman[106],
Z. Uysal[11d], V. Vacek[137], B. Vachon[100], K.O.H. Vadla[129], T. Vafeiadis[34], C. Valderanis[110],
E. Valdes Santurio[43a,43b], M. Valente[163a], S. Valentinetti[21b,21a], A. Valero[169], R.A. Vallance[19],
A. Vallier[98], J.A. Valls Ferrer[169], T.R. Van Daalen[144], P. Van Gemmeren[5], S. Van Stroud[92],
I. Van Vulpen[115], M. Vanadia[71a,71b], W. Vandelli[34], M. Vandenbroucke[140], E.R. Vandewall[125],
D. Vannicola[157], L. Vannoli[53b,53a], R. Vari[70a], E.W. Varnes[6], C. Varni[16], T. Varol[154],
D. Varouchas[62], K.E. Varvell[153], M.E. Vasile[25b], L. Vaslin[36], G.A. Vasquez[171], F. Vazeille[36],
D. Vazquez Furelos[12], T. Vazquez Schroeder[34], J. Veatch[51], V. Vecchio[97], M.J. Veen[115],
I. Veliscek[130], L.M. Veloce[162], F. Veloso[135a,135c], S. Veneziano[70a], A. Ventura[65a,65b],
A. Verbytskyi[111], M. Verducci[69a,69b], C. Vergis[22], M. Verissimo De Araujo[78b], W. Verkerke[115],
A.T. Vermeulen[115], J.C. Vermeulen[115], C. Vernieri[149], P.J. Verschuuren[91], M. Vessella[99],
M.L. Vesterbacka[121], M.C. Vetterli[148,aj], A. Vgenopoulos[158], N. Viaux Maira[142e], T. Vickey[145],
O.E. Vickey Boeriu[145], G.H.A. Viehhauser[130], L. Vigani[59b], M. Villa[21b,21a],
M. Villaplana Perez[169], E.M. Villhauer[48], E. Vilucchi[49], M.G. Vincter[32], G.S. Virdee[19],
A. Vishwakarma[48], C. Vittori[21b,21a], I. Vivarelli[152], V. Vladimirov[173], E. Voevodina[111],
M. Vogel[177], P. Vokac[137], J. Von Ahnen[44], E. Von Toerne[22], V. Vorobel[138], K. Vorobev[108],
M. Vos[169], J.H. Vossebeld[88], M. Vozak[97], L. Vozdecky[90], N. Vranjes[14],
M. Vranjes Milosavljevic[14], V. Vrba[137,*], M. Vreeswijk[115], N.K. Vu[98], R. Vuillermet[34],
O.V. Vujinovic[96], I. Vukotic[35], S. Wada[164], C. Wagner[99], W. Wagner[177], S. Wahdan[177],
H. Wahlberg[86], R. Wakasa[164], M. Wakida[112], V.M. Walbrecht[111], J. Walder[139], R. Walker[110],
S.D. Walker[91], W. Walkowiak[147], A.M. Wang[57], A.Z. Wang[176], C. Wang[58a], C. Wang[58c],
H. Wang[16], J. Wang[60a], P. Wang[40], R.-J. Wang[96], R. Wang[57], R. Wang[116], S.M. Wang[154],
S. Wang[58b], T. Wang[58a], W.T. Wang[75], W.X. Wang[58a], X. Wang[13c], X. Wang[168], X. Wang[58c],
Y. Wang[58a], Z. Wang[102], C. Wanotayaroj[34], A. Warburton[100], C.P. Ward[30], R.J. Ward[19],
N. Warrack[55], A.T. Watson[19], M.F. Watson[19], G. Watts[144], B.M. Waugh[92], A.F. Webb[10],
C. Weber[27], M.S. Weber[18], S.A. Weber[32], S.M. Weber[59a], C. Wei[58a], Y. Wei[130],

A.R. Weidberg[130], J. Weingarten[45], M. Weirich[96], C. Weiser[50], T. Wenaus[27], B. Wendland[45],
T. Wengler[34], S. Wenig[34], N. Wermes[22], M. Wessels[59a], K. Whalen[127], A.M. Wharton[87],
A.S. White[57], A. White[7], M.J. White[1], D. Whiteson[166], L. Wickremasinghe[128],
W. Wiedenmann[176], C. Wiel[46], M. Wielers[139], N. Wieseotte[96], C. Wiglesworth[38],
L.A.M. Wiik-Fuchs[50], D.J. Wilbern[124], H.G. Wilkens[34], L.J. Wilkins[91], D.M. Williams[37],
H.H. Williams[132], S. Williams[30], S. Willocq[99], P.J. Windischhofer[130], I. Wingerter-Seez[4],
F. Winklmeier[127], B.T. Winter[50], M. Wittgen[149], M. Wobisch[93], A. Wolf[96], R. Wölker[130],
J. Wollrath[166], M.W. Wolter[82], H. Wolters[135a,135c], V.W.S. Wong[170], A.F. Wongel[44],
S.D. Worm[44], B.K. Wosiek[82], K.W. Woźniak[82], K. Wraight[55], J. Wu[13a,13d], S.L. Wu[176],
X. Wu[52], Y. Wu[58a], Z. Wu[140,58a], J. Wuerzinger[130], T.R. Wyatt[97], B.M. Wynne[48], S. Xella[38],
L. Xia[13c], M. Xia[13b], J. Xiang[60c], X. Xiao[102], M. Xie[58a], X. Xie[58a], I. Xiotidis[152], D. Xu[13a],
H. Xu[58a], H. Xu[58a], L. Xu[58a], R. Xu[132], T. Xu[58a], W. Xu[102], Y. Xu[13b], Z. Xu[58b], Z. Xu[149],
B. Yabsley[153], S. Yacoob[31a], N. Yamaguchi[85], Y. Yamaguchi[160], M. Yamatani[159],
H. Yamauchi[164], T. Yamazaki[16], Y. Yamazaki[80], J. Yan[58c], S. Yan[130], Z. Yan[23], H.J. Yang[58c,58d],
H.T. Yang[16], S. Yang[58a], T. Yang[60c], X. Yang[58a], X. Yang[13a], Y. Yang[159], Z. Yang[102,58a],
W-M. Yao[16], Y.C. Yap[44], H. Ye[13c], J. Ye[40], S. Ye[27], I. Yeletskikh[77], M.R. Yexley[87], P. Yin[37],
K. Yorita[174], K. Yoshihara[76], C.J.S. Young[50], C. Young[149], M. Yuan[102], R. Yuan[58b,i], X. Yue[59a],
M. Zaazoua[33e], B. Zabinski[82], G. Zacharis[9], E. Zaid[48], A.M. Zaitsev[118,ae], T. Zakareishvili[155b],
N. Zakharchuk[32], S. Zambito[34], D. Zanzi[50], S.V. Zeißner[45], C. Zeitnitz[177], J.C. Zeng[168],
D.T. Zenger Jr[24], O. Zenin[118], T. Ženiš[26a], S. Zenz[90], S. Zerradi[33a], D. Zerwas[62], B. Zhang[13c],
D.F. Zhang[145], G. Zhang[13b], J. Zhang[5], K. Zhang[13a], L. Zhang[13c], M. Zhang[168], R. Zhang[176],
S. Zhang[102], X. Zhang[58c], X. Zhang[58b], Z. Zhang[62], P. Zhao[47], T. Zhao[58b], Y. Zhao[141],
Z. Zhao[58a], A. Zhemchugov[77], Z. Zheng[149], D. Zhong[168], B. Zhou[102], C. Zhou[176], H. Zhou[6],
N. Zhou[58c], Y. Zhou[6], C.G. Zhu[58b], C. Zhu[13a,13d], H.L. Zhu[58a], H. Zhu[13a], J. Zhu[102], Y. Zhu[58a],
X. Zhuang[13a], K. Zhukov[107], V. Zhulanov[117b,117a], D. Zieminska[63], N.I. Zimine[77],
S. Zimmermann[50,*], J. Zinsser[59b], M. Ziolkowski[147], L. Živković[14], A. Zoccoli[21b,21a], K. Zoch[52],
T.G. Zorbas[145], O. Zormpa[42], W. Zou[37], L. Zwalinski[34]

1   *Department of Physics, University of Adelaide, Adelaide, Australia*

2   *Department of Physics, University of Alberta, Edmonton AB, Canada*

3   *(a) Department of Physics, Ankara University, Ankara; (b) Istanbul Aydin University, Application and Research Center for Advanced Studies, Istanbul; (c) Division of Physics, TOBB University of Economics and Technology, Ankara, Turkey*

4   *LAPP, Univ. Savoie Mont Blanc, CNRS/IN2P3, Annecy, France*

5   *High Energy Physics Division, Argonne National Laboratory, Argonne IL, United States of America*

6   *Department of Physics, University of Arizona, Tucson AZ, United States of America*

7   *Department of Physics, University of Texas at Arlington, Arlington TX, United States of America*

8   *Physics Department, National and Kapodistrian University of Athens, Athens, Greece*

9   *Physics Department, National Technical University of Athens, Zografou, Greece*

10   *Department of Physics, University of Texas at Austin, Austin TX, United States of America*

11   *(a) Bahcesehir University, Faculty of Engineering and Natural Sciences, Istanbul; (b) Istanbul Bilgi University, Faculty of Engineering and Natural Sciences, Istanbul; (c) Department of Physics, Bogazici University, Istanbul; (d) Department of Physics Engineering, Gaziantep University, Gaziantep, Turkey*

12   *Institut de Física d'Altes Energies (IFAE), Barcelona Institute of Science and Technology, Barcelona, Spain*

13   *(a) Institute of High Energy Physics, Chinese Academy of Sciences, Beijing; (b) Physics Department, Tsinghua University, Beijing; (c) Department of Physics, Nanjing University, Nanjing; (d) University of Chinese Academy of Science (UCAS), Beijing, China*

14   *Institute of Physics, University of Belgrade, Belgrade, Serbia*

[15] Department for Physics and Technology, University of Bergen, Bergen, Norway

[16] Physics Division, Lawrence Berkeley National Laboratory and University of California, Berkeley CA, United States of America

[17] Institut für Physik, Humboldt Universität zu Berlin, Berlin, Germany

[18] Albert Einstein Center for Fundamental Physics and Laboratory for High Energy Physics, University of Bern, Bern, Switzerland

[19] School of Physics and Astronomy, University of Birmingham, Birmingham, United Kingdom

[20] [a] Facultad de Ciencias y Centro de Investigaciónes, Universidad Antonio Nariño, Bogotá; [b] Departamento de Física, Universidad Nacional de Colombia, Bogotá, Colombia

[21] [a] Dipartimento di Fisica e Astronomia A. Righi, Università di Bologna, Bologna; [b] INFN Sezione di Bologna, Italy

[22] Physikalisches Institut, Universität Bonn, Bonn, Germany

[23] Department of Physics, Boston University, Boston MA, United States of America

[24] Department of Physics, Brandeis University, Waltham MA, United States of America

[25] [a] Transilvania University of Brasov, Brasov; [b] Horia Hulubei National Institute of Physics and Nuclear Engineering, Bucharest; [c] Department of Physics, Alexandru Ioan Cuza University of Iasi, Iasi; [d] National Institute for Research and Development of Isotopic and Molecular Technologies, Physics Department, Cluj-Napoca; [e] University Politehnica Bucharest, Bucharest; [f] West University in Timisoara, Timisoara, Romania

[26] [a] Faculty of Mathematics, Physics and Informatics, Comenius University, Bratislava; [b] Department of Subnuclear Physics, Institute of Experimental Physics of the Slovak Academy of Sciences, Kosice, Slovak Republic

[27] Physics Department, Brookhaven National Laboratory, Upton NY, United States of America

[28] Departamento de Física (FCEN) and IFIBA, Universidad de Buenos Aires and CONICET, Buenos Aires, Argentina

[29] California State University, CA, United States of America

[30] Cavendish Laboratory, University of Cambridge, Cambridge, United Kingdom

[31] [a] Department of Physics, University of Cape Town, Cape Town; [b] iThemba Labs, Western Cape; [c] Department of Mechanical Engineering Science, University of Johannesburg, Johannesburg; [d] National Institute of Physics, University of the Philippines Diliman (Philippines); [e] University of South Africa, Department of Physics, Pretoria; [f] School of Physics, University of the Witwatersrand, Johannesburg, South Africa

[32] Department of Physics, Carleton University, Ottawa ON, Canada

[33] [a] Faculté des Sciences Ain Chock, Réseau Universitaire de Physique des Hautes Energies - Université Hassan II, Casablanca; [b] Faculté des Sciences, Université Ibn-Tofail, Kénitra; [c] Faculté des Sciences Semlalia, Université Cadi Ayyad, LPHEA-Marrakech; [d] LPMR, Faculté des Sciences, Université Mohamed Premier, Oujda; [e] Faculté des sciences, Université Mohammed V, Rabat; [f] Mohammed VI Polytechnic University, Ben Guerir, Morocco

[34] CERN, Geneva, Switzerland

[35] Enrico Fermi Institute, University of Chicago, Chicago IL, United States of America

[36] LPC, Université Clermont Auvergne, CNRS/IN2P3, Clermont-Ferrand, France

[37] Nevis Laboratory, Columbia University, Irvington NY, United States of America

[38] Niels Bohr Institute, University of Copenhagen, Copenhagen, Denmark

[39] [a] Dipartimento di Fisica, Università della Calabria, Rende; [b] INFN Gruppo Collegato di Cosenza, Laboratori Nazionali di Frascati, Italy

[40] Physics Department, Southern Methodist University, Dallas TX, United States of America

[41] Physics Department, University of Texas at Dallas, Richardson TX, United States of America

[42] National Centre for Scientific Research "Demokritos", Agia Paraskevi, Greece

[43] [a] Department of Physics, Stockholm University; [b] Oskar Klein Centre, Stockholm, Sweden

[44] Deutsches Elektronen-Synchrotron DESY, Hamburg and Zeuthen, Germany

[45] Fakultät Physik, Technische Universität Dortmund, Dortmund, Germany

[46] Institut für Kern- und Teilchenphysik, Technische Universität Dresden, Dresden, Germany

[47] Department of Physics, Duke University, Durham NC, United States of America

48 *SUPA - School of Physics and Astronomy, University of Edinburgh, Edinburgh, United Kingdom*

49 *INFN e Laboratori Nazionali di Frascati, Frascati, Italy*

50 *Physikalisches Institut, Albert-Ludwigs-Universität Freiburg, Freiburg, Germany*

51 *II. Physikalisches Institut, Georg-August-Universität Göttingen, Göttingen, Germany*

52 *Département de Physique Nucléaire et Corpusculaire, Université de Genève, Genève, Switzerland*

53 [a]*Dipartimento di Fisica, Università di Genova, Genova;* [b]*INFN Sezione di Genova, Italy*

54 *II. Physikalisches Institut, Justus-Liebig-Universität Giessen, Giessen, Germany*

55 *SUPA - School of Physics and Astronomy, University of Glasgow, Glasgow, United Kingdom*

56 *LPSC, Université Grenoble Alpes, CNRS/IN2P3, Grenoble INP, Grenoble, France*

57 *Laboratory for Particle Physics and Cosmology, Harvard University, Cambridge MA, United States of America*

58 [a]*Department of Modern Physics and State Key Laboratory of Particle Detection and Electronics, University of Science and Technology of China, Hefei;* [b]*Institute of Frontier and Interdisciplinary Science and Key Laboratory of Particle Physics and Particle Irradiation (MOE), Shandong University, Qingdao;* [c]*School of Physics and Astronomy, Shanghai Jiao Tong University, Key Laboratory for Particle Astrophysics and Cosmology (MOE), SKLPPC, Shanghai;* [d]*Tsung-Dao Lee Institute, Shanghai, China*

59 [a]*Kirchhoff-Institut für Physik, Ruprecht-Karls-Universität Heidelberg, Heidelberg;* [b]*Physikalisches Institut, Ruprecht-Karls-Universität Heidelberg, Heidelberg, Germany*

60 [a]*Department of Physics, Chinese University of Hong Kong, Shatin, N.T., Hong Kong;* [b]*Department of Physics, University of Hong Kong, Hong Kong;* [c]*Department of Physics and Institute for Advanced Study, Hong Kong University of Science and Technology, Clear Water Bay, Kowloon, Hong Kong, China*

61 *Department of Physics, National Tsing Hua University, Hsinchu, Taiwan*

62 *IJCLab, Université Paris-Saclay, CNRS/IN2P3, 91405, Orsay, France*

63 *Department of Physics, Indiana University, Bloomington IN, United States of America*

64 [a]*INFN Gruppo Collegato di Udine, Sezione di Trieste, Udine;* [b]*ICTP, Trieste;* [c]*Dipartimento Politecnico di Ingegneria e Architettura, Università di Udine, Udine, Italy*

65 [a]*INFN Sezione di Lecce;* [b]*Dipartimento di Matematica e Fisica, Università del Salento, Lecce, Italy*

66 [a]*INFN Sezione di Milano;* [b]*Dipartimento di Fisica, Università di Milano, Milano, Italy*

67 [a]*INFN Sezione di Napoli;* [b]*Dipartimento di Fisica, Università di Napoli, Napoli, Italy*

68 [a]*INFN Sezione di Pavia;* [b]*Dipartimento di Fisica, Università di Pavia, Pavia, Italy*

69 [a]*INFN Sezione di Pisa;* [b]*Dipartimento di Fisica E. Fermi, Università di Pisa, Pisa, Italy*

70 [a]*INFN Sezione di Roma;* [b]*Dipartimento di Fisica, Sapienza Università di Roma, Roma, Italy*

71 [a]*INFN Sezione di Roma Tor Vergata;* [b]*Dipartimento di Fisica, Università di Roma Tor Vergata, Roma, Italy*

72 [a]*INFN Sezione di Roma Tre;* [b]*Dipartimento di Matematica e Fisica, Università Roma Tre, Roma, Italy*

73 [a]*INFN-TIFPA;* [b]*Università degli Studi di Trento, Trento, Italy*

74 *Institut für Astro- und Teilchenphysik, Leopold-Franzens-Universität, Innsbruck, Austria*

75 *University of Iowa, Iowa City IA, United States of America*

76 *Department of Physics and Astronomy, Iowa State University, Ames IA, United States of America*

77 *Joint Institute for Nuclear Research, Dubna, Russia*

78 [a]*Departamento de Engenharia Elétrica, Universidade Federal de Juiz de Fora (UFJF), Juiz de Fora;* [b]*Universidade Federal do Rio De Janeiro COPPE/EE/IF, Rio de Janeiro;* [c]*Instituto de Física, Universidade de São Paulo, São Paulo, Brazil*

79 *KEK, High Energy Accelerator Research Organization, Tsukuba, Japan*

80 *Graduate School of Science, Kobe University, Kobe, Japan*

81 [a]*AGH University of Science and Technology, Faculty of Physics and Applied Computer Science, Krakow;* [b]*Marian Smoluchowski Institute of Physics, Jagiellonian University, Krakow, Poland*

82 *Institute of Nuclear Physics Polish Academy of Sciences, Krakow, Poland*

83 *Faculty of Science, Kyoto University, Kyoto, Japan*

84   *Kyoto University of Education, Kyoto, Japan*

85   *Research Center for Advanced Particle Physics and Department of Physics, Kyushu University, Fukuoka, Japan*

86   *Instituto de Física La Plata, Universidad Nacional de La Plata and CONICET, La Plata, Argentina*

87   *Physics Department, Lancaster University, Lancaster, United Kingdom*

88   *Oliver Lodge Laboratory, University of Liverpool, Liverpool, United Kingdom*

89   *Department of Experimental Particle Physics, Jožef Stefan Institute and Department of Physics, University of Ljubljana, Ljubljana, Slovenia*

90   *School of Physics and Astronomy, Queen Mary University of London, London, United Kingdom*

91   *Department of Physics, Royal Holloway University of London, Egham, United Kingdom*

92   *Department of Physics and Astronomy, University College London, London, United Kingdom*

93   *Louisiana Tech University, Ruston LA, United States of America*

94   *Fysiska institutionen, Lunds universitet, Lund, Sweden*

95   *Departamento de Física Teorica C-15 and CIAFF, Universidad Autónoma de Madrid, Madrid, Spain*

96   *Institut für Physik, Universität Mainz, Mainz, Germany*

97   *School of Physics and Astronomy, University of Manchester, Manchester, United Kingdom*

98   *CPPM, Aix-Marseille Université, CNRS/IN2P3, Marseille, France*

99   *Department of Physics, University of Massachusetts, Amherst MA, United States of America*

100   *Department of Physics, McGill University, Montreal QC, Canada*

101   *School of Physics, University of Melbourne, Victoria, Australia*

102   *Department of Physics, University of Michigan, Ann Arbor MI, United States of America*

103   *Department of Physics and Astronomy, Michigan State University, East Lansing MI, United States of America*

104   *B.I. Stepanov Institute of Physics, National Academy of Sciences of Belarus, Minsk, Belarus*

105   *Research Institute for Nuclear Problems of Byelorussian State University, Minsk, Belarus*

106   *Group of Particle Physics, University of Montreal, Montreal QC, Canada*

107   *P.N. Lebedev Physical Institute of the Russian Academy of Sciences, Moscow, Russia*

108   *National Research Nuclear University MEPhI, Moscow, Russia*

109   *D.V. Skobeltsyn Institute of Nuclear Physics, M.V. Lomonosov Moscow State University, Moscow, Russia*

110   *Fakultät für Physik, Ludwig-Maximilians-Universität München, München, Germany*

111   *Max-Planck-Institut für Physik (Werner-Heisenberg-Institut), München, Germany*

112   *Graduate School of Science and Kobayashi-Maskawa Institute, Nagoya University, Nagoya, Japan*

113   *Department of Physics and Astronomy, University of New Mexico, Albuquerque NM, United States of America*

114   *Institute for Mathematics, Astrophysics and Particle Physics, Radboud University/Nikhef, Nijmegen, The Netherlands*

115   *Nikhef National Institute for Subatomic Physics and University of Amsterdam, Amsterdam, The Netherlands*

116   *Department of Physics, Northern Illinois University, DeKalb IL, United States of America*

117   *[a] Budker Institute of Nuclear Physics and NSU, SB RAS, Novosibirsk; [b] Novosibirsk State University Novosibirsk, Russia*

118   *Institute for High Energy Physics of the National Research Centre Kurchatov Institute, Protvino, Russia*

119   *Institute for Theoretical and Experimental Physics named by A.I. Alikhanov of National Research Centre "Kurchatov Institute", Moscow, Russia*

120   *[a] New York University Abu Dhabi, Abu Dhabi; [b] United Arab Emirates University, Al Ain; [c] University of Sharjah, Sharjah, United Arab Emirates*

121   *Department of Physics, New York University, New York NY, United States of America*

122   *Ochanomizu University, Otsuka, Bunkyo-ku, Tokyo, Japan*

123   *Ohio State University, Columbus OH, United States of America*

124   *Homer L. Dodge Department of Physics and Astronomy, University of Oklahoma, Norman OK, United States of America*

125   *Department of Physics, Oklahoma State University, Stillwater OK, United States of America*

126   *Palacký University, Joint Laboratory of Optics, Olomouc, Czech Republic*

127   *Institute for Fundamental Science, University of Oregon, Eugene, OR, United States of America*

128   *Graduate School of Science, Osaka University, Osaka, Japan*

129   *Department of Physics, University of Oslo, Oslo, Norway*

130   *Department of Physics, Oxford University, Oxford, United Kingdom*

131   *LPNHE, Sorbonne Université, Université Paris Cité, CNRS/IN2P3, Paris, France*

132   *Department of Physics, University of Pennsylvania, Philadelphia PA, United States of America*

133   *Konstantinov Nuclear Physics Institute of National Research Centre "Kurchatov Institute", PNPI, St. Petersburg, Russia*

134   *Department of Physics and Astronomy, University of Pittsburgh, Pittsburgh PA, United States of America*

135   [a]*Laboratório de Instrumentação e Física Experimental de Partículas - LIP, Lisboa;* [b]*Departamento de Física, Faculdade de Ciências, Universidade de Lisboa, Lisboa;* [c]*Departamento de Física, Universidade de Coimbra, Coimbra;* [d]*Centro de Física Nuclear da Universidade de Lisboa, Lisboa;* [e]*Departamento de Física, Universidade do Minho, Braga;* [f]*Departamento de Física Teórica y del Cosmos, Universidad de Granada, Granada (Spain);* [g]*Instituto Superior Técnico, Universidade de Lisboa, Lisboa, Portugal*

136   *Institute of Physics of the Czech Academy of Sciences, Prague, Czech Republic*

137   *Czech Technical University in Prague, Prague, Czech Republic*

138   *Charles University, Faculty of Mathematics and Physics, Prague, Czech Republic*

139   *Particle Physics Department, Rutherford Appleton Laboratory, Didcot, United Kingdom*

140   *IRFU, CEA, Université Paris-Saclay, Gif-sur-Yvette, France*

141   *Santa Cruz Institute for Particle Physics, University of California Santa Cruz, Santa Cruz CA, United States of America*

142   [a]*Departamento de Física, Pontificia Universidad Católica de Chile, Santiago;* [b]*Instituto de Investigación Multidisciplinario en Ciencia y Tecnología, y Departamento de Física, Universidad de La Serena;* [c]*Universidad Andres Bello, Department of Physics, Santiago;* [d]*Instituto de Alta Investigación, Universidad de Tarapacá, Arica;* [e]*Departamento de Física, Universidad Técnica Federico Santa María, Valparaíso, Chile*

143   *Universidade Federal de São João del Rei (UFSJ), São João del Rei, Brazil*

144   *Department of Physics, University of Washington, Seattle WA, United States of America*

145   *Department of Physics and Astronomy, University of Sheffield, Sheffield, United Kingdom*

146   *Department of Physics, Shinshu University, Nagano, Japan*

147   *Department Physik, Universität Siegen, Siegen, Germany*

148   *Department of Physics, Simon Fraser University, Burnaby BC, Canada*

149   *SLAC National Accelerator Laboratory, Stanford CA, United States of America*

150   *Department of Physics, Royal Institute of Technology, Stockholm, Sweden*

151   *Departments of Physics and Astronomy, Stony Brook University, Stony Brook NY, United States of America*

152   *Department of Physics and Astronomy, University of Sussex, Brighton, United Kingdom*

153   *School of Physics, University of Sydney, Sydney, Australia*

154   *Institute of Physics, Academia Sinica, Taipei, Taiwan*

155   [a]*E. Andronikashvili Institute of Physics, Iv. Javakhishvili Tbilisi State University, Tbilisi;* [b]*High Energy Physics Institute, Tbilisi State University, Tbilisi, Georgia*

156   *Department of Physics, Technion, Israel Institute of Technology, Haifa, Israel*

157   *Raymond and Beverly Sackler School of Physics and Astronomy, Tel Aviv University, Tel Aviv, Israel*

158   *Department of Physics, Aristotle University of Thessaloniki, Thessaloniki, Greece*

159   *International Center for Elementary Particle Physics and Department of Physics, University of Tokyo, Tokyo, Japan*

160   *Department of Physics, Tokyo Institute of Technology, Tokyo, Japan*

161   *Tomsk State University, Tomsk, Russia*

162   *Department of Physics, University of Toronto,*
      Toronto ON, Canada

163   (a) *TRIUMF, Vancouver BC;* (b) *Department of Physics and Astronomy, York University, Toronto*
      ON, Canada

164   *Division of Physics and Tomonaga Center for the History of the Universe, Faculty of Pure and*
      Applied Sciences, University of Tsukuba, Tsukuba, Japan

165   *Department of Physics and Astronomy, Tufts University, Medford MA, United States of America*

166   *Department of Physics and Astronomy, University of California Irvine, Irvine CA,*
      United States of America

167   *Department of Physics and Astronomy, University of Uppsala, Uppsala, Sweden*

168   *Department of Physics, University of Illinois, Urbana IL, United States of America*

169   *Instituto de Física Corpuscular (IFIC), Centro Mixto Universidad de Valencia - CSIC, Valencia,*
      Spain

170   *Department of Physics, University of British Columbia, Vancouver BC, Canada*

171   *Department of Physics and Astronomy, University of Victoria, Victoria BC, Canada*

172   *Fakultät für Physik und Astronomie, Julius-Maximilians-Universität Würzburg, Würzburg, Germany*

173   *Department of Physics, University of Warwick, Coventry, United Kingdom*

174   *Waseda University, Tokyo, Japan*

175   *Department of Particle Physics and Astrophysics, Weizmann Institute of Science, Rehovot, Israel*

176   *Department of Physics, University of Wisconsin, Madison WI, United States of America*

177   *Fakultät für Mathematik und Naturwissenschaften, Fachgruppe Physik, Bergische Universität*
      Wuppertal, Wuppertal, Germany

178   *Department of Physics, Yale University, New Haven CT, United States of America*

a   *Also at Borough of Manhattan Community College, City University of New York, New York NY,*
    United States of America

b   *Also at Bruno Kessler Foundation, Trento, Italy*

c   *Also at Center for High Energy Physics, Peking University, China*

d   *Also at Centro Studi e Ricerche Enrico Fermi, Italy*

e   *Also at CERN, Geneva, Switzerland*

f   *Also at Département de Physique Nucléaire et Corpusculaire, Université de Genève, Genève,*
    Switzerland

g   *Also at Departament de Fisica de la Universitat Autonoma de Barcelona, Barcelona, Spain*

h   *Also at Department of Financial and Management Engineering, University of the Aegean, Chios,*
    Greece

i   *Also at Department of Physics and Astronomy, Michigan State University, East Lansing MI,*
    United States of America

j   *Also at Department of Physics and Astronomy, University of Louisville, Louisville, KY,*
    United States of America

k   *Also at Department of Physics, Ben Gurion University of the Negev, Beer Sheva, Israel*

l   *Also at Department of Physics, California State University, East Bay, United States of America*

m   *Also at Department of Physics, California State University, Fresno, United States of America*

n   *Also at Department of Physics, California State University, Sacramento, United States of America*

o   *Also at Department of Physics, King's College London, London, United Kingdom*

p   *Also at Department of Physics, St. Petersburg State Polytechnical University, St. Petersburg, Russia*

q   *Also at Department of Physics, University of Fribourg, Fribourg, Switzerland*

r   *Also at Faculty of Physics, M.V. Lomonosov Moscow State University, Moscow, Russia*

s   *Also at Faculty of Physics, Sofia University, 'St. Kliment Ohridski', Sofia, Bulgaria*

t   *Also at Graduate School of Science, Osaka University, Osaka, Japan*

u   *Also at Hellenic Open University, Patras, Greece*

v   *Also at Institucio Catalana de Recerca i Estudis Avancats, ICREA, Barcelona, Spain*

^w Also at Institut für Experimentalphysik, Universität Hamburg, Hamburg, Germany

^x Also at Institute for Particle and Nuclear Physics, Wigner Research Centre for Physics, Budapest, Hungary

^y Also at Institute of Particle Physics (IPP), Canada

^z Also at Institute of Physics, Azerbaijan Academy of Sciences, Baku, Azerbaijan

^{aa} Also at Institute of Theoretical Physics, Ilia State University, Tbilisi, Georgia

^{ab} Also at Instituto de Fisica Teorica, IFT-UAM/CSIC, Madrid, Spain

^{ac} Also at Istanbul University, Dept. of Physics, Istanbul, Turkey

^{ad} Also at Joint Institute for Nuclear Research, Dubna, Russia

^{ae} Also at Moscow Institute of Physics and Technology State University, Dolgoprudny, Russia

^{af} Also at National Research Nuclear University MEPhI, Moscow, Russia

^{ag} Also at Physics Department, An-Najah National University, Nablus, Palestine

^{ah} Also at Physikalisches Institut, Albert-Ludwigs-Universität Freiburg, Freiburg, Germany

^{ai} Also at The City College of New York, New York NY, United States of America

^{aj} Also at TRIUMF, Vancouver BC, Canada

^{ak} Also at Università di Napoli Parthenope, Napoli, Italy

^{al} Also at University of Chinese Academy of Sciences (UCAS), Beijing, China

^{am} Also at Yeditepe University, Physics Department, Istanbul, Turkey

[*] Deceased